© 2015. Published by The Company of Biologists Ltd | Development (2015) 142, 4056-4067 doi:10.1242/dev.128298

RESEARCH ARTICLE

Hoxc8 initiates an ectopic mammary program by regulating *Fgf10* and *Tbx3* expression and Wnt/β-catenin signaling

Lara S. Carroll[1,*] and Mario R. Capecchi[2]

ABSTRACT

The role of Hox genes in the formation of cutaneous accessory organs such as hair follicles and mammary glands has proved elusive, a likely consequence of overlapping function and expression among various homeobox factors. Lineage and immunohistochemical analysis of *Hoxc8* in mice revealed that this midthoracic Hox gene has transient but strong regional expression in ventrolateral surface ectoderm at E10.5, much earlier than previously reported. Targeted mice were generated to conditionally misexpress *Hoxc8* from the *Rosa* locus using select *Cre* drivers, which significantly expanded the domain of thoracic identity in mutant embryos. Accompanying this expansion was the induction of paired zones of ectopic mammary development in the cervical region, which generated between three and five pairs of mammary placodes anterior to the first wild-type mammary rudiment. These rudiments expressed the mammary placode markers *Wnt10b* and *Tbx3* and were labeled by antibodies to the mammary mesenchyme markers ERα and androgen receptor. Somitic *Fgf10* expression, which is required for normal mammary line formation, was upregulated in mutant cervical somites, and conditional ablation of ectodermal *Tbx3* expression eliminated all normally positioned and ectopic mammary placodes. We present evidence that *Hoxc8* participates in regulating the initiation stages of mammary placode morphogenesis, and suggest that this and other Hox genes are likely to have important roles during regional specification and initiation of these and other cutaneous accessory organs.

KEY WORDS: *Hoxc8*, Wnt signaling, *Tbx3*, *Fgf10*, Mammary placodes, Vibrissae, Skin appendages, Mouse

INTRODUCTION

During embryonic development, the epidermis and underlying dermis of vertebrate skin collaborate via respective epithelial and mesenchymal signals to create cutaneous appendages, such as hair and feather follicles, mammary glands, teeth and sweat glands. Despite the morphological and functional differences among mature skin organs, each begins as a placode, a raised epithelial thickening that initiates in response to a broadly expressed Wnt signal from the dermis (Mikkola, 2007). As mammary and hair placodes begin to develop and invade the mesenchyme, dermal and epidermal Wnt signaling continues, along with additional signaling molecules such as fibroblast growth factors (FGFs), bone morphogenetic proteins (BMPs), ectodysplasin (Eda-A1) and sonic hedgehog (Shh) to effect specific development of each organ type (Andl et al., 2002; Chu et al., 2004; Gallego et al., 2002; Mikkola and Millar, 2006; Mustonen et al., 2004; Petiot et al., 2003; Plikus et al., 2004; St-Jacques et al., 1998; Veltmaat, 2013; Zhang et al., 2009).

In mice, the first visible sign of mammary development is the appearance at E10.5 of two histologically distinct lines of pseudostratified ectoderm between the forelimb and hindlimb buds, marked by *Wnt10b* expression (Veltmaat et al., 2004). This ectoderm is a permissive region for mammary rudiments (MRs) 2, 3 and 4, joining additional streaks of mammary permissive ectoderm in the axial and inguinal regions giving rise to MRs 1 and 5 (Veltmaat et al., 2004). Ectopic mammary glands occur most commonly at inappropriate sites along these lines. Evidence in rabbits and mice suggests that mammary placodes form by migration of epithelial cells into and along the mammary lines, resulting in the five pairs of MRs developing non-sequentially at characteristic positions along the body axis (Lee et al., 2011; Propper, 1978). Molecular requirements differ among the pairs of mammary placodes, and differential gene expression profiles may underlie some of the heterogeneous attributes and susceptibilities to tumor incidence in adult mammary glands (Veltmaat et al., 2013).

Proper positioning of the mammary line along the dorsoventral axis is achieved in part by mutual antagonism between ventrally expressed *Bmp4* and the more dorsally expressed T-box transcription factor *Tbx3* (Cho et al., 2006; Veltmaat et al., 2006). These and additional mammary factors, such as *Gli3*, retinoic acid, *Nrg3* and *Fgf10*, play important roles in the appropriate patterning of Wnt signals that are required to achieve the proper rostrocaudal positioning of placodes (Cho et al., 2012; Cowin and Wysolmerski, 2010; Hatsell and Cowin, 2006; Howard, 2008; Lee et al., 2013; Mailleux et al., 2002; Veltmaat et al., 2006).

The idea that a 'HOX code' (Kessel and Gruss, 1991) might underlie the regional distribution of cutaneous appendages has been around since the discovery that Hox gene expression exhibits positional variation within the skin itself (Bieberich et al., 1991; Chuong, 1993). The majority of Hox genes appear to be expressed in fetal or adult skin and hair follicles (Awgulewitsch, 2003; Johansson and Headon, 2014), and several Hox genes are expressed in developing and mature mammary glands, or become dysregulated during mammary neoplasia (Chen and Sukumar, 2003; Hayashida et al., 2010; Lewis, 2000; Wu et al., 2006). During early embryogenesis, expression of vertebrate Hox genes initiates in a rostral to caudal direction along the body axis in a sequence mirroring the linear position of each gene within the four chromosomal Hox clusters, a unique feature termed 'spatiotemporal colinearity'. Each cell along the Hox trajectory receives a distinct combination of Hox proteins, a HOX code (Kessel and Gruss, 1991) that may uniquely specify its position, patterning individual elements from the hindbrain to the most posterior vertebrae. However, unlike axial Hox expression, only a subset of the tested Hox genes have been shown to exhibit regional restriction of expression within mouse, human or chick embryonic skin, including *Hoxc8*, *Hoxb4*, *Hoxa7*, *Hoxd9*, *Hoxd11* and *Hoxd13*

[1]Moran Eye Center, University of Utah, Salt Lake City, UT 84132, USA. [2]Department of Human Genetics and Howard Hughes Medical Institute, University of Utah, Salt Lake City, UT 84112, USA.

*Author for correspondence (lsc3@utah.edu)

Received 9 July 2015; Accepted 1 October 2015

Development (2015) 142, 4056-4067 doi:10.1242/dev.128298

(Kanzler et al., 1994; Reid and Gaunt, 2002). Several others, including *Hoxc13*, which has a crucial role in hair shaft development, are expressed broadly throughout the epidermis and/or dermis (Godwin and Capecchi, 1998; Kanzler et al., 1994; Reid and Gaunt, 2002). Therefore, Hox gene temporal and spatial expression in embryonic skin does not strictly match the colinear expression found in axial Hox domains, and the putative HOX code responsible for globally defining domains of emerging epidermal organs has proved elusive, a likely consequence of the complex combinatorial nature of Hox expression and function.

The strongest evidence for Hox-mediated regional patterning of epidermal organs comes from two thoracic Hox genes. Adult thoracic mammary glands of mice lacking functional *Hoxc6* are devoid of mammary epithelium, whereas inguinal mammary glands develop ductal structures and are less severely affected (Garcia-Gasca and Spyropoulos, 2000). *Hoxc8* has been indirectly implicated in the specification of feather and hair types (Kanzler et al., 1997; Mentzer et al., 2008) and, in mice, *Hoxc8* shows regionally restricted expression during the first wave of hair placodogenesis, the earliest reported expression of any Hox gene in the epidermis (Johansson and Headon, 2014; Kanzler et al., 1994).

Using a Hoxc8IresCre mouse line (Chen et al., 2010), we found *Hoxc8* lineage in mammary line ectoderm by E10.75 and that it was incorporated into all five MRs by E12.5. This result prompted us to carefully re-examine *Hoxc8* expression in embryonic skin in order to assess the potential of this Hox gene to mediate early skin regionalization and skin appendage specification. Further analysis demonstrated transient regionally specific expression of Hoxc8 protein in the ectoderm during mammary line formation, prior to the earliest reported *Hoxc8* ectodermal expression. We tested the possibility that *Hoxc8* expression plays a role in mammary line specification using mice carrying a targeted allele designed to conditionally express *Hoxc8*. Conditional misexpression of *Hoxc8* using two out of three *Cre* drivers consistently led to the appearance of supernumerary MRs within two distinct domains: along the normal mammary line of mutant mice, and within the cervical region anterior to the first MR. These ectopic rudiments express the placode markers *Bmp2*, *Wnt10b* and *Tbx3* and are labeled by the mammary mesenchyme-specific markers ERα and androgen receptor.

This study is the first to implicate a Hox gene in rostrocaudal positioning of mammary line ectoderm and placodes. We present evidence that *Hoxc8* positively regulates *Tbx3* and *Fgf10* expression and Wnt/β-catenin signaling and, moreover, that *Tbx3* is a direct Hoxc8 transcriptional target. These data further support the existence of a HOX code underlying regional specification of embryonic skin at the earliest stages of skin placode initiation.

RESULTS

Hoxc8 is transiently expressed in ventrolateral flank ectoderm prior to formation of the mammary line

Hoxc8 is cited as one of the first Hox genes expressed in embryonic mouse skin, with its earliest reported expression in E14.5 epidermis (Awgulewitsch, 2003; Johansson and Headon, 2014; Kanzler et al., 1994). Lineage analysis and Hoxc8 antibody were both employed to re-examine cutaneous Hoxc8 expression to determine if it is appropriately staged to play a role in the early specification of mammary glands. Lineage was examined using a Hoxc8IresCre mouse line (Chen et al., 2010) and either RosaYFP or RosalacZ (C8cre/YFP and C8cre/lacZ) (Soriano, 1999). The C8cre/YFP lineage at E12.5 is broadly represented throughout flank caudal to the forelimb bud (n=3). The reporter additionally labels all MRs (Fig. 1A, MR1 is obscured by the forelimb), revealing that Hoxc8 protein is also expressed in early surface ectoderm and may be present in ectodermal precursors giving rise to mammary epithelium. Hoxc8 antibody did not label E13.5 mammary bud ectoderm (Fig. 1B; data not shown; n=3), indicating that ectodermal Hoxc8 is transitory, preceding the mammary bud stage.

To pinpoint the timing and extent of transient *Hoxc8* expression, we next examined the Hoxc8 lineage in sectioned C8cre/lacZ embryos (in which all *Hoxc8*-expressing cells and descendants are labeled), and subsequently examined transient expression in wild-type embryo sections labeled with Hoxc8 antibody (Fig. 1C-F; data not shown; two or three embryos were examined at each time point indicated). The *lacZ* reporter extends rostrally in E10.75 ventrolateral ectoderm to the forelimb level encompassing the region of the developing mammary line between forelimb and hindlimb (Fig. 1C). At a slightly earlier stage, Hoxc8 antibody labels all surface ectoderm extending between and including the forelimb and hindlimb buds of E10.5 embryos, which necessarily includes the rostrocaudal extent of the forming mammary line (Fig. 1D; data not shown). By E11.5 and E12.5, ectodermal expression of Hoxc8 is considerably reduced, particularly in the epithelium of the forming mammary placodes and buds (Fig. 1E,F). *In situ* hybridization of wild-type embryos with a *Hoxc8* probe (Fig. 1G; n=2) shows expression in E11.5 hypaxial extensions of thoracic somites, which include S15 and S16, underlying the portion of the mammary line specifically giving rise to MR3 (Veltmaat et al., 2006).

Rostral expansion of mammary ectoderm in A3cre/CAGC8 embryos accompanies expansion of thoracic vertebral identity

The paraxial and surface ectodermal expression of Hoxc8 make it an ideal candidate for a potential role in mediating mammary line and third placode specification. We shifted the domains of *Hoxc8* paraxial, mesodermal, and ectodermal expression using the Hoxa3IresCre mouse (Macatee et al., 2003) to test if Hoxc8 misexpression could alter mammary line and placode positioning. The E10.5 A3cre/lacZ lineage shows widespread expression throughout lateral mesoderm and somites (the rostral expression limit of somitic Hoxa3 corresponds to the first cervical vertebrae) and much of the body ectoderm caudal to the second branchial arch (Fig. 2A; n=3). A3cre/CAGC8 embryos express ectopic Hoxc8 wherever the IresEGFP signal is present in a pattern equivalent to the A3cre/lacZ lineage. This fluorescent signal was subsequently used to genotype A3cre/CAGC8 mutants (Fig. 2B).

In contrast to the wild-type pattern of 13 thoracic ribs seen in control embryos, mutant A3cre/CAGC8 embryos exhibited well-formed ectopic ribs on all cervical, lumbar and sacral vertebrae as well as rib-like extensions on several caudal vertebrae (Fig. 2C,D; n=6). This phenotype is 100% penetrant in A3cre/CAGC8 mutants and is consistent with previous studies demonstrating a fundamental role of Hox genes in assigning anteroposterior vertebral identity (Carapuço et al., 2005; Le Mouellic et al., 1992; McIntyre et al., 2007; van den Akker et al., 2001; Wellik and Capecchi, 2003). The cervical region appears elongated in A3cre/CAGC8 mutants, which is likely to be related to its transformation to a thoracic identity. Interestingly, we found that the rib phenotype is dependent on *Hoxc8* dosage, as a nearly identical construct minus the potent CAGGS promoter (also targeted to the *Rosa* locus, driven only by the *Rosa* promoter) yielded only mild skeletal phenotypes, consistent with a previously reported *Hoxc8* transgenic mutant (Pollock et al., 1992) (Fig. S1; n=16).

Development (2015) 142, 4056-4067 doi:10.1242/dev.128298

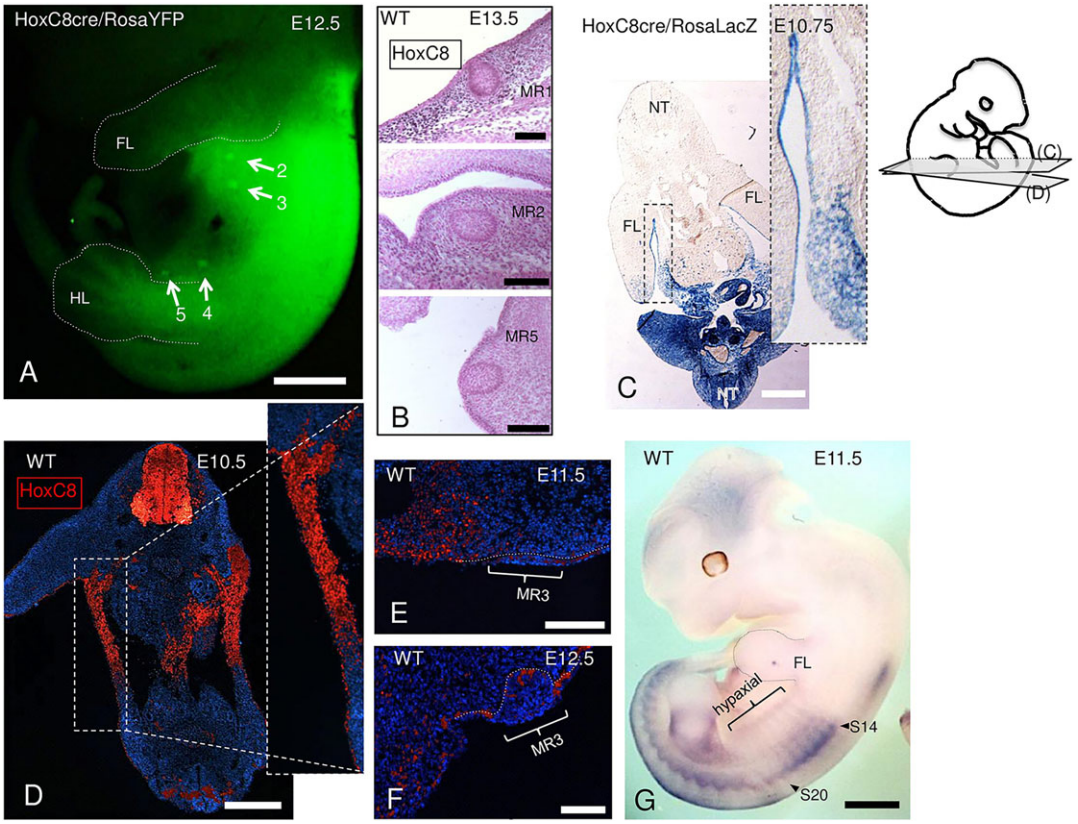

Fig. 1. *Hoxc8* lineage and expression. (A) *Hoxc8* lineage of an E12.5 C8cre/YFP mouse embryo includes all mammary buds (numbered arrows). The first mammary rudiment (MR) is obscured by the forelimb. (B) 10 µm sagittal sections through MRs 1, 2 and 5 of E13.5 wild-type embryos labeled with Hoxc8 antibody (black nuclear stain). (C,D) Embryos are sectioned approximately along the planes indicated in the drawing. (C) *Hoxc8* lineage (β-gal signal) in ventrolateral surface ectoderm. (D) Hoxc8 antibody (red) labels E10.5 ventrolateral surface ectoderm extending between and including both limb buds. (E) Hoxc8 is almost absent from mammary placodes by E11.5, and from the surface ectoderm by E12.5 (ectodermal/mesenchymal boundary indicated by dotted line) (F). (G) *Hoxc8*-expressing somites and hypaxial extensions in a wild-type E11.5 embryo. FL, forelimb; HL, hindlimb; NT, neural tube; S, somite; WT, wild type. Scale bars: 1 mm in A,G; 500 µm in C,D; 100 µm in B,E,F.

The dermomyotome, marked by *Myf5* expression, exhibited ectopic hypaxial extensions within the cervical and lumbar regions of E11.5 A3cre/CAGC8 embryos (Fig. 2E,F; n=3). We used *Bmp2* as a general placode marker, as its expression focally marks the epithelium of the mammary bud (Phippard et al., 1996), hair (Suzuki et al., 2009) vibrissae, tooth (Bitgood and McMahon, 1995), and tongue papillae (Jung et al., 1999). At E11.5, we found that A3cre/CAGC8 embryos exhibited strong upregulation of *Bmp2*. Focal *Bmp2* expression was seen within irregularly spaced placodes in the cervical ectoderm, with dark streaks of *Bmp2* signal along the normal mammary line (Fig. 2G,H; n=3). Control embryos exhibited only faint streaks of ectodermal *Bmp2* expression along the mammary line, punctuated by focal upregulation within MR3, the first MR to form. We next examined expression of three of the earliest known genes associated with mammary line/placode formation: *Fgf10*, *Tbx3* and *Wnt10b* (Fig. 2I-R; $n\geq3$ per genotype per time point for each probe). Formation of placodes 1, 2, 3 and 5 requires *Fgf10* expression, which emanates from thoracic somites. Homozygous ablation of *Fgf10*, or of its ectodermal receptor *Fgfr2b*, results in the absence of all four placodes (Mailleux et al., 2002; Veltmaat et al., 2006). *Fgf10* signal appears upregulated in cervical and thoracic somites of A3cre/CAGC8 mutant embryos at E10.5 compared with control littermates (Fig. 2I,J, Fig. S2A,B). Other domains of *Fgf10* expression, including limb buds, appear unchanged in the mutants.

Tbx3 is required for the formation of mammary buds 1, 3, 4 and 5 (Davenport et al., 2003; Eblaghie et al., 2004; Veltmaat, 2013). In humans, heterozygous mutation of *TBX3* causes ulnar-mammary syndrome, characterized by upper limb, genital, mammary and other glandular defects (Bamshad et al., 1999). In both control and A3cre/CAGC8 E10.5 mouse embryos, *Tbx3* is expressed in a broad strip of lateral plate mesoderm underlying the mammary line, and in another broad region of lateral mesoderm extending caudally from the fourth pharyngeal arch to the forelimb (Fig. 2K,L). By E11.5, *Tbx3* levels in control embryos have greatly decreased in the cervical lateral mesoderm, but remain high in the A3cre/CAGC8 mutant, as a continuum extending from the hindlimb through thoracic and cervical levels (Fig. 2M,N, Fig. S2C,D). Focal *Tbx3* upregulation in mutant cervical placodes is obvious by this stage. However, in the mammary line ectoderm, mutant *Tbx3* signal persists as a streak, whereas placode formation in controls is nearly complete (Fig. 2M,N). Notably, ectopic cervical placodes are not restricted to a linear pattern, in contrast to supernumerary placodes developing within the mammary line. At E13.5 strong *Tbx3* expression is confined to the ten mammary buds in controls, whereas mutants (with 100% penetrance) exhibit strong *Tbx3* expression in both normally positioned mammary buds and supernumerary buds along the mammary line and in the ectopic cervical zone. We generally found one or two *Tbx3*-expressing ectopic buds occurring within each E13.5 mammary line, and as many as 12 ectopic cervical buds in a single A3cre/CAGC8 embryo (Fig. 2O,P). Ectodermal *Wnt10b* (Fig. 2Q,R, Fig. S2E,F) shows a pattern of dysregulation remarkably similar to that of *Tbx3* and *Bmp2* in E11.5 mutant embryos. Because

Development (2015) 142, 4056-4067 doi:10.1242/dev.128298

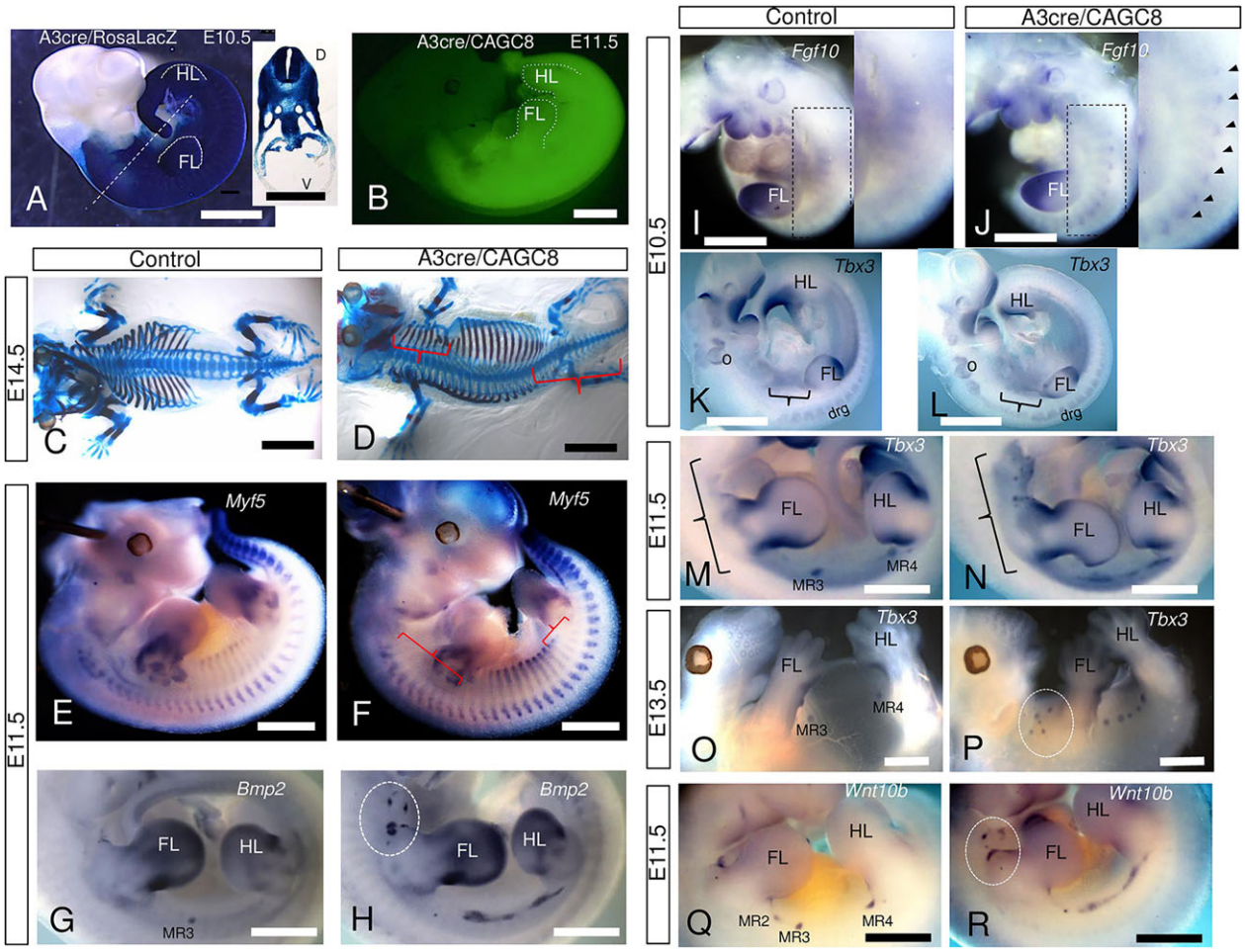

Fig. 2. Mammary placode markers are ectopically expressed in the expanded thoracic region of A3cre/CAGC8 embryos. (A) *Hoxa3* lineage in an A3cre/lacZ E10.5 embryo. Inset is a 70 µm vibratome section through the region indicated by the dashed line (D, dorsal; V, ventral). (B) *Hoxa3* lineage in an E11.5 A3cre/CAGC8(IresEGFP) embryo marks the domain of *Hoxc8* misexpression. (C,D) Control and A3cre/CAGC8 mutant E14.5 skeletal preps. Red brackets indicate the formation of ectopic ribs. (E,F) Expression of *Myf5* in E11.5 control (E) and A3cre/CAGC8 (F) embryos. Red brackets show ectopic hypaxial expression. (G,H) *Bmp2* expression in control (G) and mutant (H) E11.5 embryos. (I,J) *Fgf10* expression in E10.5 control and A3cre/CAGC8 embryos. Arrowheads in the inset (J) show upregulated expression in cervical somites. (K,L) *Tbx3* expression in E10.5 control (K) and A3cre/CAGC8 (L) embryos. Brackets indicate *Tbx3* signal in lateral cervical mesoderm and pharyngeal arches. drg, dorsal root ganglia; o, otic vesicle. (M,N) *Tbx3* expression in E11.5 control (M) and A3cre/CAGC8 (N) embryos. Brackets indicate anterior extension of lateral mesoderm (part of the forelimb is damaged in N). (O,P) *Tbx3* expression in E13.5 mammary buds of control (O) and A3cre/CAGC8 (P) embryos. (Q,R) *Wnt10b* expression in placodes and mammary line of E11.5 control (Q) and A3cre/CAGC8 (R) embryos. Dotted ovals indicate cervical mammary placodes/buds. Scale bars: 2 mm in C,D; 1 mm in all other panels.

A3cre/CAGC8 embryos die at or around E14.5, later stages of mutant mammary development cannot be examined without orthotopic transplantation.

Somitic Hoxc8 misexpression results in supernumerary placode formation within the mammary line

We next induced Hoxc8 misexpression with Pax3cre (Engleka et al., 2005) in order to determine whether ectopic somitic *Hoxc8* is sufficient to generate an anterior mammary permissive zone. In E11.5 Pax3cre/lacZ embryos, β-gal marks the dorsal neural tube and strongly labels somites and hypaxial dermomyotome (Fig. 3A,B; n=2). Importantly, *lacZ* is not expressed in body surface ectoderm (Fig. 3B, inset), allowing us to test the competence of *Hoxc8* in establishing an ectopic mammary permissive zone via its expression within somitic derivatives only. Like A3cre/CAGC8 embryos, Pax3cre/CAGC8 embryos died at or around E14.5. By E14.0, well-formed ribs were established on all cervical vertebrae and the first three lumbar vertebrae of Pax3cre/CAGC8 embryos, whereas embryos carrying only the *Pax3*^{cre} allele produced the wild-type rib formula (Fig. 3C,D; n=6). Transformation of cervical vertebrae to a thoracic identity was accompanied by upregulation of the mammary factors *Fgf10* and *Tbx3* in hypaxial extensions of Pax3cre/CAGC8 cervical somites (Fig. 3E-H; n=3 per genotype per probe). However, in contrast to A3cre/CAGC8 mutants, neither *Tbx3* nor *Bmp2* (n=2) expression showed focal upregulation in the cervical ectoderm of Pax3cre/CAGC8 mutants (Fig. 3G-J).

Wnt/β-catenin signaling was examined in E13.5 Pax3cre/CAGC8 mice using the TOPgal reporter (DasGupta and Fuchs, 1999). Consistent with the absence of *Tbx3* and *Bmp2* expression in cervical placodes, no focal spots of high TOPgal expression were found anterior to MR1 in Pax3cre/CAGC8 mutants at E13.5 (Fig. 3K,L; n=7), suggesting the absence of ectopic cervical MR formation in these mutants. These results indicate that although ectopic *Hoxc8* within somites is sufficient to expand thoracic vertebral identity into the cervical region, it is insufficient to expand the zone of permissive mammary-forming ectoderm. On the other hand, four out of seven mutant embryos (57%) formed a single unilateral supernumerary mammary bud between MR3 and MR4 in

Development (2015) 142, 4056-4067 doi:10.1242/dev.128298

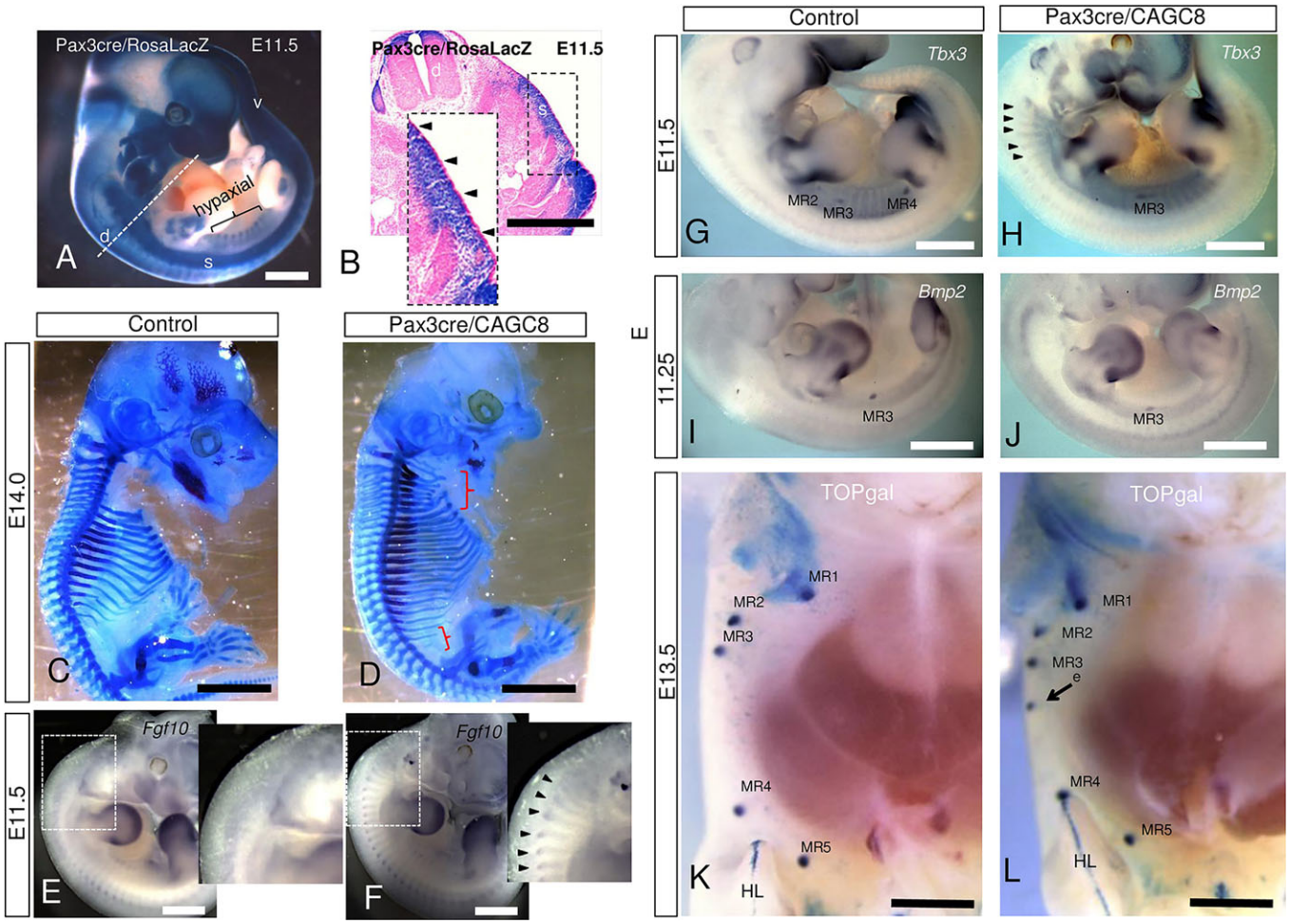

Fig. 3. Pax3cre/CAGC8 mutants have expanded thoracic identity, but do not develop cervical placodes. (A) *Pax3* lineage in a whole-mount E11.5 Pax3cre/lacZ embryo. (B) 12 µm paraffin transverse section of the β-gal-stained embryo in A at level of the dashed line. Arrowheads in the inset show lack of signal in the surface ectoderm. d, dorsal; v, ventral; s, somite. (C,D) Control and Pax3cre/CAGC8 mutant E14 skeletal preparations. Red brackets show ectopic ribs. (E,F) *Fgf10* expression in E11.5 control (E) and Pax3cre/CAGC8 (F) embryos. Arrowheads in the inset show upregulated expression in central somites and hypaxial extensions. (G,H) *Tbx3* expression in E11.5 control and Pax3cre/CAGC8 embryos. Arrowheads show ectopic expression in hypaxial extensions of cervical somites. (I,J) *Bmp2* expression in E11.25 control (I) and Pax3cre/CAGC8 (J) embryos. (K,L) Frontal views of whole-mount E13.5 TOPgal control (K) and TOPgal/Pax3cre/CAGC8 (L) embryos stained for β-gal. Heads and forelimbs are removed for clarity. The arrow points to a single supernumerary mammary bud (e). Scale bars: 1 mm in A,E-L; 500 µm in B; 2 mm in C,D.

addition to all normally positioned MRs (Fig. 3K,L). This location overlies the hypaxial domain of endogenous *Hoxc8* expression (Fig. 1G) and suggests that an increased level of somitic *Hoxc8* can promote mammary placode development as long as it underlies a region of ectoderm that is competent for mammary formation.

Simultaneous Hoxc8 misexpression in somites and overlying ectoderm establishes a cervical zone of mammary ectoderm

To test whether simultaneous *Hoxc8* expression in ectoderm and somitic derivatives is sufficient to recapitulate the anterior zone of cervical mammary placodes found in A3cre/CAGC8 mutants, we misexpressed *Hoxc8* using a Wnt6cre driver (N. Makki, PhD Thesis, University of Utah, 2010). *Wnt6* is initially expressed in a broad band of ectoderm encompassing the mammary-forming region, and becomes restricted to the developing mammary placodes (Veltmaat et al., 2004). Analysis of E10.5 W6cre/lacZ embryos showed *Wnt6* lineage extending across most of the surface ectoderm prior to mammary line formation (Fig. 4A and inset; n=3), although the *Wnt6* lineage was considerably weaker within lateral mesoderm compared with the *Hoxa3* lineage. Dermomyotomal expression of *Wnt6* is restricted to the dorsomedial lip (Ikeya and Takada, 1998). Consequently, hypaxial signal (which derives from dorsolateral dermomyotome) was not detectable in *Wnt6* lineage of W6cre/lacZ control embryos (Fig. 4A), or in *Wnt6* lineage of W6cre/CAGC8 mutants (as visualized by the IresEGFP reporter; Fig. 4B), indicating that ectopic *Hoxc8* is restricted to non-hypaxial somite in this conditional cross.

Unlike A3cre/CAGC8 and Pax3cre/CAGC8 embryos, W6cre/CAGC8 embryos survive until birth, but die perinatally. We found rudimentary or fully formed ectopic ribs on one or two cervical vertebrae of W6cre/CAGC8 mutants (Fig. 4C,D; n=6), suggesting that hypaxial *Hoxc8* expression is not required for transformation of cervical somites towards a thoracic identity. Somitic *Hoxc8* expression was accompanied by upregulation of *Fgf10* expression in cervical somites by E10.5 (Fig. 4E,F; n=4).

Expression patterns and levels of *Tbx3* were nearly equivalent between control and W6cre/CAGC8 littermates at E10.5 (Fig. 4G,H; n=4), similar to A3cre/CAGC8 embryos and littermates at this stage. By E11.5, *Tbx3* expression was focally upregulated in cervical ectoderm of Wnt6cre/CAGC8 mutants with 100%

Development (2015) 142, 4056-4067 doi:10.1242/dev.128298

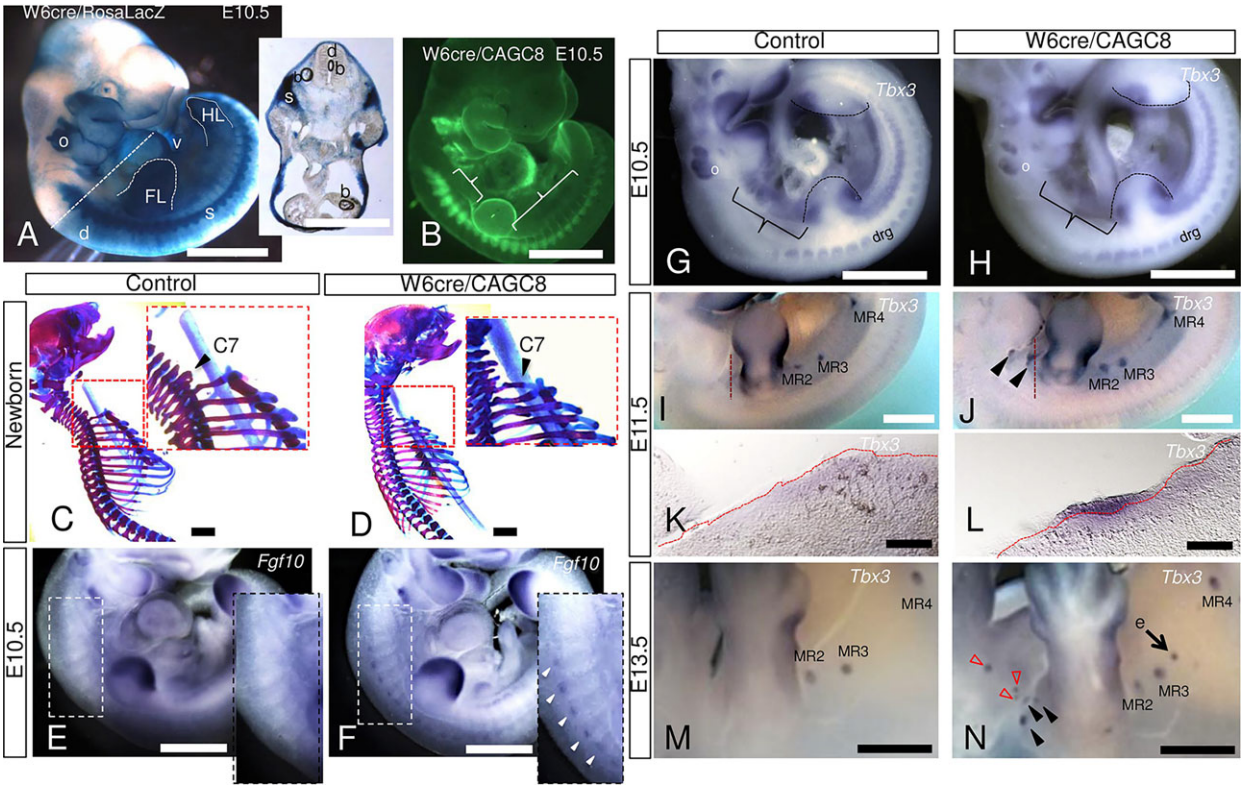

Fig. 4. Supernumerary MRs develop in cervical and mammary line ectoderm of W6cre/CAGC8 embryos. (A) *Wnt6* lineage in an E10.5 W6cre/RosalacZ embryo. Inset shows a 70 µm vibratome transverse section through the region demarcated by the dotted line. Three bubbles (b) are trapped in this section. (B) *Wnt6* lineage in an E10.5 W6cre/CAGC8(IresEGFP) embryo identifies the domain of *Hoxc8* misexpression. Brackets indicate lack of *Wnt6* lineage in hypaxial extensions. (C,D) Newborn control embryo and W6cre/CAGC8 embryo showing mutant cervical ribs (arrowhead). (E,F) *Fgf10* expression in E10.5 control (E) and W6cre/CAGC8 (F) embryos. Arrowheads in the inset show elevated expression in mutant cervical somites. (G,H) *Tbx3* expression in E10.5 control and W6cre/CAGC8 embryos. Brackets indicate signal in cervical and pharyngeal arch mesoderm. (I,J) *Tbx3* expression in E11.5 control (I) and W6cre/CAGC8 (J) embryos. Arrowheads show focal upregulation in cervical ectoderm. (K,L) 70 µm vibratome transverse sections through the regions indicated by dotted lines in I,J. Red dotted lines demarcate the mesodermal-ectodermal border. (M,N) *Tbx3* expression in E13.5 control (M) and W6cre/CAGC8 (N) embryos. Black arrowheads (N) indicate ectopic cervical MRs. A supernumerary rudiment has formed along the mammary line (e, arrow). Red arrowheads indicate accessory vibrissal placodes with aberrant *Tbx3* signal. Scale bars: 1 mm in A,B,E-J,M,N; 2 mm in C,D; 100 µm in K,L.

penetrance, indicating the formation of ectopic placodes (Fig. 4I-L; n=4). Whereas *Tbx3* expression is aberrantly maintained in the cervical mesoderm of A3cre/CAGC8 mutant embryos at E11.5 (Fig. 2K,L), *Tbx3* expression in W6cre/CAGC8 cervical mesoderm is similar to that in controls at this stage (Fig. 4G-J). Within the wild-type mammary line, *Tbx3* expression in control embryos was confined to placodes by E11.5, whereas W6cre/CAGC8 embryos exhibited lingering expression along the mammary line, and considerably broader, more diffuse expression within the forming placodes themselves (Fig. 4I,J). By E13.5, *Tbx3* expression was focally restricted to mammary buds in both controls and mutants (Fig. 4M,N; n=4). W6cre/CAGC8 mutants had fewer ectopic buds at E13.5 than A3cre/CAGC8 mutants, with an average of one ectopic bud in each mammary line and up to eight extra buds anterior to MR1.

At E13.5, Tbx3 antibody labeled all mammary bud epithelium (including supernumerary MRs), the surrounding mammary mesenchyme, and scattered cells in the underlying mesoderm (Fig. 5A,B; n=4). In serial sections of the same E13.5 embryos, Hoxc8 antibody labeled mutant epidermis and mammary primordia, as well as scattered cells in the underlying mesoderm (Fig. 1A, Fig. 5C,D; n=4), but was only present in scattered mesoderm of controls. We verified the mammary identity of ectopic cervical placodes in E13.5 W6cre/CAGC8 embryos by labeling mammary mesenchyme with antibodies for estrogen receptor alpha (ERα; Esr1 – Mouse Genome Informatics) (n=2) and androgen receptor (n=3). All supernumerary as well as normally positioned mammary placodes expressed both markers in control and mutant embryos (Fig. 5E-H; data not shown). We found that *Tbx3* expression was aberrantly upregulated in the epithelium of E13.5 W6cre/CAGC8 vibrissae at E13.5 relative to controls (Fig. 4M,N; Fig. S3A,B), leading us to speculate that vibrissal placodes might be adopting a mammary fate. However, neither ERα nor androgen receptor antibody labeled mesenchyme of the vibrissal placodes of control or W6cre/CAGC8 embryos (Fig. S3C,D; data not shown; n=3) indicating that, although vibrissal structures are incorrectly specified, ectopic *Hoxc8* and consequent *Tbx3* misexpression does not direct vibrissal differentiation towards a mammary program.

Wnt/β-catenin signaling is abnormally upregulated in mammary placode epithelium of W6cre/CAGC8 embryos

As Wnt signaling is essential for the initiation and subsequent development of all ectodermal organs (Boras-Granic and Hamel, 2013; Chu et al., 2004; Lim and Nusse, 2013), we performed a detailed timeline of TOPgal reporter expression at different embryonic stages to study changes in Wnt signaling that accompany *Hoxc8* dysregulation. W6cre/CAGC8 embryos survive until birth, enabling us to perform TOPgal analysis during mammary ductal elongation and branching. In E10.5 embryos, TOPgal reporter expression was consistently expanded in W6cre/

Development (2015) 142, 4056-4067 doi:10.1242/dev.128298

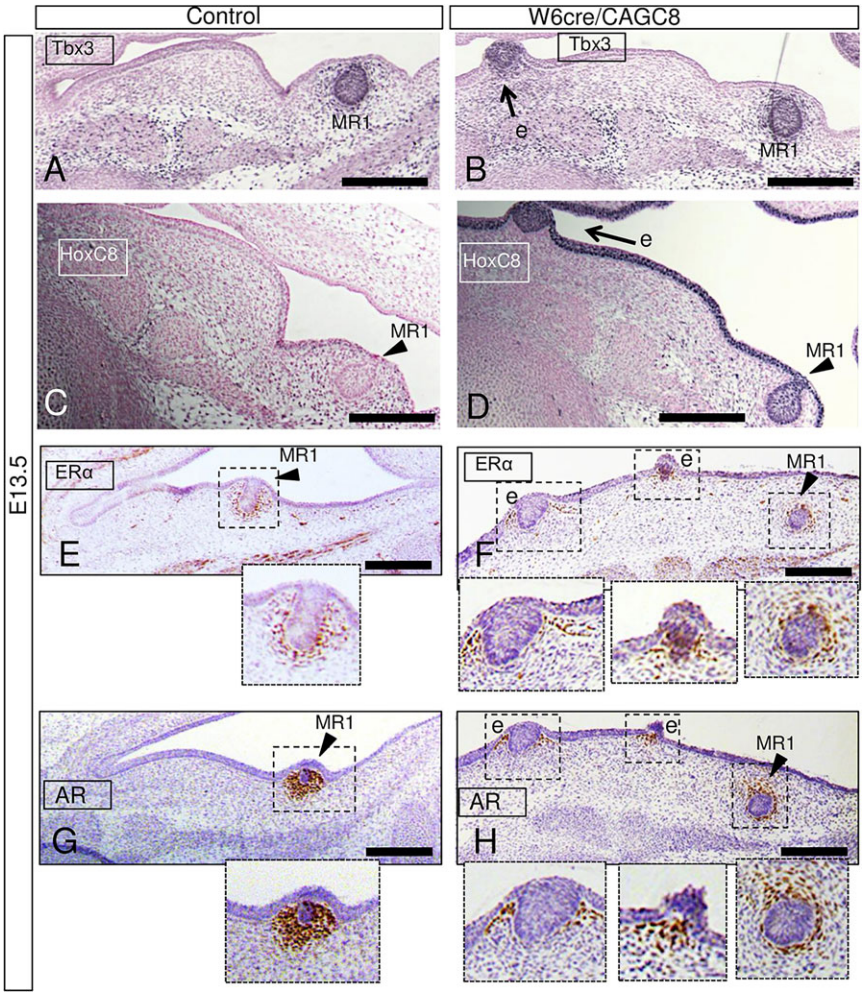

Fig. 5. Ectopic cervical rudiments express mammary-specific markers. Parasagittal sections through the cervical/axillary region of E13.5 control (A,C,E,G) and W6cre/CAGC8 (B,D,F,H) embryos, immunolabeled for Tbx3 (A,B), Hoxc8 (C,D) and the mammary-specific mesenchyme markers ERα (E,F) and androgen receptor (AR) (G,H). e, ectopic cervical rudiments anterior to MR1. (A-D) Black antibody signal counterstained with nuclear Fast Red. (E-H) Brown (DAB) antibody signal counterstained with a 3-second Hematoxylin dip. Scale bars: 200 µm.

CAGC8 cervical lateral mesoderm relative to control littermates (Fig. 6A,B; *n*=6), with expression extending rostrally to the fourth branchial arch. Limb and mammary line ectoderm showed similar faint staining between mutants and controls (Fig. 6A,B). Interestingly, the cervical pattern of Wnt/β-catenin signaling at E10.5 completely overlapped with *Tbx3* expression at the same embryonic stage (Fig. 4G,H). At E11.5, the cervical TOPgal signal became more localized to the neck-forelimb junction. Vibratome sections through this region show considerably stronger signal in the mutant ectoderm and mesoderm compared with controls (Fig. 6C,D; *n*=4). Placode patterning along the wild-type mammary lines of E11.5 control embryos appeared as focal aggregations of β-gal-positive cells. However, Wnt signaling in the mutant showed ostensibly delayed aggregation of β-gal-positive cells into mammary placodes. (Fig. 6C,D). Placode aggregation of *Wnt10b*-expressing cells in W6cre/CAGC8 embryos at E11.5 paralleled the delay seen with TOPgal expression (Fig. S4; *n*=2).

At E12.5, both mutant and control embryos displayed diffuse patches of β-gal-positive mesoderm caudal to the ear and in the cervical region. However, in the mutant, these diffusely stained patches contained focal spots stained dark blue, representing ectopic mammary primordia (Fig. 6E,F; *n*=6), which resolve by E13.5 into three or four ectopic mammary buds anterior to MR1 on both sides (Fig. 6G-J; *n*=8). At E13.5, these ectopic buds often protruded abnormally from the ectoderm (Fig. 6H, top inset), but by E15.5 have invaginated into the underlying dermis, as do MRs along the mammary line (Fig. 6K,L,Q,R; *n*=3). Approximately 60% of E12.5 and E13.5 W6cre/CAGC8C8 mutant mice bore one or two small supernumerary mammary buds located between MR3 and MR4 (Fig. 6E,F). Normally positioned mammary buds of E12.5 and E13.5 W6cre/CAGC8 mutants always appeared larger than those of control littermates (as opposed to the ectopic buds, which were usually smaller than endogenous buds), and by E13.5 MR3 was situated proximally and fused to MR2 in nearly half of all mutant embryos (Fig. 6H). Supernumerary, fused, and normally positioned mammary buds all expressed the downstream Wnt transcription factor Lef1 (*n*=3) in mammary epithelium (Fig. 6G,H insets; data not shown).

By E15.5, Wnt/β-catenin signaling in controls is downregulated in the neck and surface epithelium overlying the growing mammary sprout. However, mammary sprouts of female W6cre/CAGC8 embryos often failed to downregulate Wnt/β-catenin signaling properly, particularly in the proximal part of MRs 2 and 3 that had fused or developed in close proximity (Fig. 6K,L). In preparations of E17.5 whole skin stained for β-gal, MRs of control embryos could be seen growing into the underlying secondary mammary mesenchyme (mammary fat pad) and branching into a primitive ductal tree. The ductal systems of all examined W6cre/CAGC8 MRs failed to develop substantially beyond the mammary sprout stage (Fig. 6M,N; *n*=3), and appeared to degenerate by birth. However, both control and mutant females were born with external nipples at anteroposterior positions that corresponded to embryonic MR

Development (2015) 142, 4056-4067 doi:10.1242/dev.128298

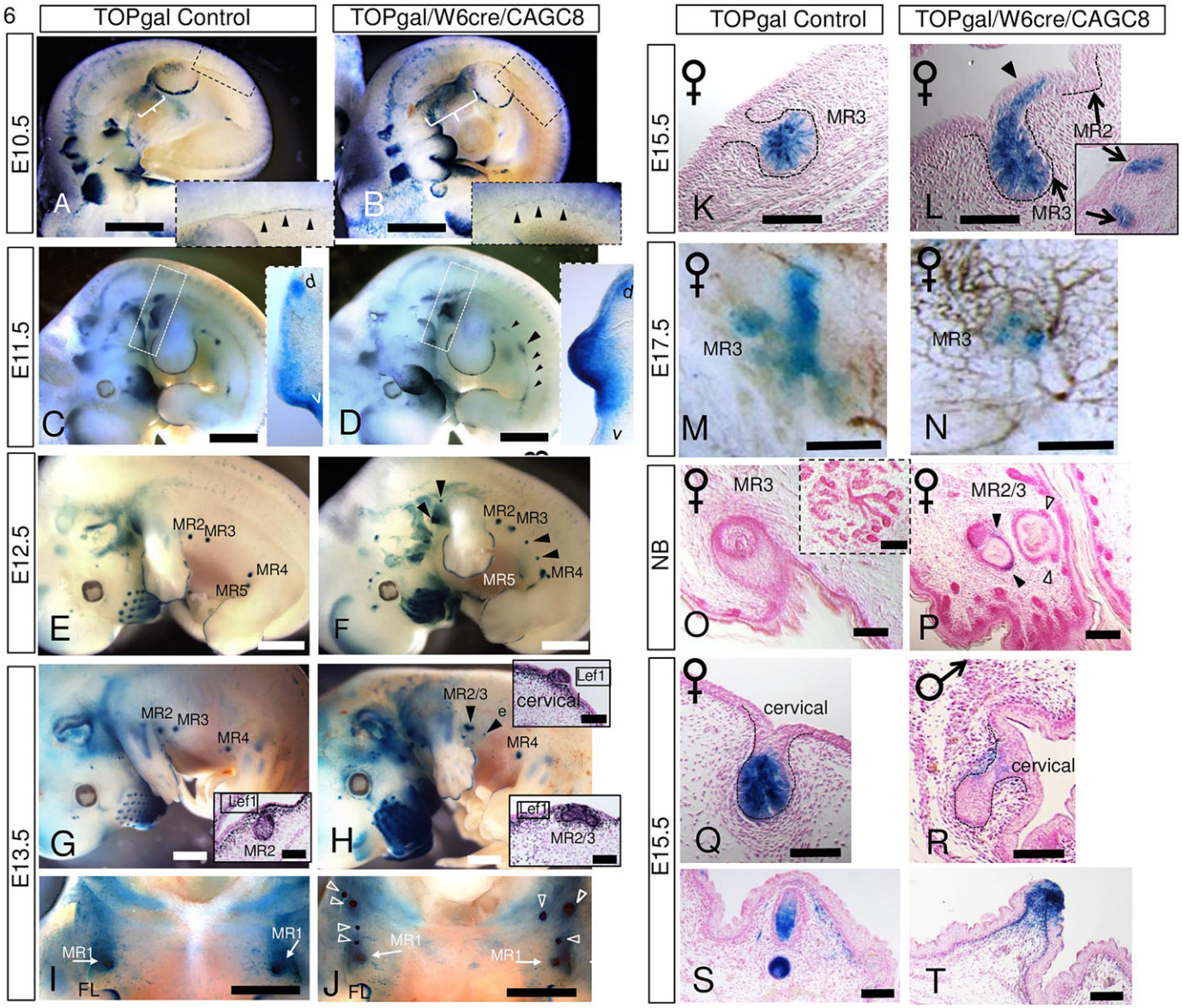

Fig. 6. Wnt/β-catenin signaling during MR development. (A,B) Brackets show upregulated TOPgal signal in the cervical region of E10.5 W6cre/CAGC8 embryos (B) compared with controls (A). Insets show faint signal along the mammary line (arrowheads). (C,D) An apparent delay of placode assembly (arrowheads) is observed in E11.5 W6cre/CAGC8 embryos (D) relative to controls (C). Insets show 70 µm vibratome transverse sections through equivalent levels within the boxed regions. (E,F) TOPgal signal in E12.5 control (E) and W6cre/CAGC8 (F) embryos. Arrowheads show supernumerary mammary buds. (G-J) TOPgal signal in E13.5 control (G,I) and W6cre/CAGC8 (H,J) embryos. Black arrowheads (H) point to an ectopic mammary bud (e) and to the fusion between mutant MR2 and MR3. Frontal views (I,J) show MR1 (arrows) and seven ectopic MRs anterior to MR1 in the mutant (arrowheads). Insets (G,H,J) show sections of E13.5 mammary buds labeled with antibody to the Wnt target Lef1. (K,L) TOPgal signal in 12 µm sections through E15.5 control and W6cre/CAGC8 mammary sprouts. Arrowhead identifies Wnt signal in ectoderm overlying mutant MRs 2 and 3 (arrows). The inset (L) is a serial section from the same embryo. (M,N) TOPgal signal in E17.5 whole-mount skin showing defective branching in the mutant (N) ductal tree compared with the control (M). (O,P) 12 µm sections of control (O) and mutant (P) newborn nipples. The inset (O) is a serial section through the same gland showing ductal branching. Black and white arrowheads (P) show defective Wnt/β-catenin signaling and hair follicle placement, respectively, in nipple epithelium. (Q,R) TOPgal signal in 12 µm sagittal sections through an ectopic mammary sprout in the cervical regions of E15.5 female (Q) and male (R) W6cre/CAGC8 embryos. (S,T) TOPgal signal in 12 µm sagittal sections though E15.5 control (S) and mutant (T) genal vibrissal follicles. All sections are counterstained with nuclear Fast Red. Scale bars: 1 mm in A-J main panels; 100 µm in K-T and insets in G,H.

formation (Fig. 6O,P; *n*=3). In newborn controls, small mammary trees were associated with nipples, whereas mutant nipples were not associated with secondary mammary mesenchyme and lacked underlying ductal branches. Interestingly, nipples of mutant newborns maintained epithelial TOPgal signal and often had hair follicles associated with nipple epithelium (Fig. 6O,P). Moreover, both female and male W6cre/CAGC8 mutants maintained mammary sprout development after E14.5 within the cervical region (Fig. 6Q,R; *n*=3 each for females and males). By contrast, all MRs along the mammary line underwent regression at E14.5 in mutant males (*n*=3), as is normal in wild-type male embryos (data not shown). Pelage hair placode and follicle morphology was normal in W6cre/CAGC8 mutant embryos (our unpublished observations). However, mutant vibrissal and whisker morphology was defective and TOPgal expression was aberrantly upregulated in vibrissal placodes by E12.5 (Fig. 6E-H,S,T).

Development (2015) 142, 4056-4067 doi:10.1242/dev.128298

Ectodermal *Tbx3* ablation abolishes both ectopic and normal MR formation

To determine the requirement of ectodermal *Tbx3* in the formation of the anterior ectopic mammary zone, we misexpressed Hoxc8 while simultaneously ablating *Tbx3* expression in the *Wnt6* domain. *Wnt6* lineage is strongly expressed in ectoderm, but is excluded from hypaxial dermomyotome, with restricted expression in lateral mesoderm prior to mammary placode formation (Fig. 4A,B). Consequently, all embryos with conditional ablation of one or both *Tbx3* alleles maintained strong *Tbx3* expression in hypaxial and lateral mesoderm, whereas no evidence of ectodermal *Tbx3* expression was found in E11.5 W6cre/Tbx3$^{\Delta/\Delta}$ or W6cre/CAGC8/Tbx3$^{\Delta/\Delta}$ embryos (Fig. 7A-D; $n \geq 4$ for each genotype). One functional copy of ectodermal *Tbx3* was sufficient to induce MR formation in W6cre/Tbx3$^{\Delta/+}$ and W6cre/CAGC8/Tbx3$^{\Delta/+}$ embryos, with cervically localized rudiments forming (with 100% penetrance) in the latter (Fig. 7C,D). Wnt/β-catenin signaling was examined in W6cre/CAGC8 E13.5 embryos with one or both *Tbx3* alleles conditionally deleted. TOPgal expression was present in cervical mammary buds of all W6cre/CAGC8/Tbx3$^{\Delta/+}$/TOPgal embryos (Fig. 7E,F; n=7), but was lost in all W6cre/CAGC8/Tbx3$^{\Delta/\Delta}$/TOPgal embryos (Fig. 7G; n=6). This establishes an ectoderm-specific requirement for *Tbx3* for mammary potentiation along the entire anteroposterior axis. In contrast to MRs, facial vibrissae and whisker pads were maintained in the absence of ectodermal *Tbx3* (Fig. 7E-G), affirming the divergent developmental trajectories of these two ectodermal appendages in response to ectopic *Hoxc8*.

We performed chromatin immunoprecipitation (ChIP) on control E11.5 embryos to determine whether Hoxc8 is capable of direct transcriptional regulation of the *Tbx3* promoter. A single primer set, located 1.5 kb 5′ of the *Tbx3* ATG start codon, amplified Hoxc8-bound chromatin from both dorsal tissue (somites and neural tube) and ventrolateral thoracic tissue (mammary line ectoderm and mesoderm), but failed to amplify IgG-immunoprecipitated chromatin from either (supplementary Materials and Methods, Fig. S5). The experiment was successfully repeated on equivalent tissues derived from E11.5 W6cre/CAGC8 embryos, suggesting that *Tbx3* might be directly regulated by Hoxc8 during mammary development of both control and mutant animals.

DISCUSSION

Somitic *Hoxc8* misexpression instigates a rib-forming program and upregulates the somitic mammary factor *Fgf10*

We used a gene targeting approach to respecify thoracic identity in somites and surface ectoderm in order to test the competence of Hoxc8-regulated factors to potentiate mammary ectoderm and initiate placode formation. Expansion of the thoracic boundary was apparent in all of our mutant crosses by the appearance of ectopic ribs on cervical and other vertebrae. Accompanying the expansion of thoracic identity, we observed the consistent upregulation of somitic *Fgf10* by ectopic *Hoxc8* in all three of our conditional mutant crosses. *Fgf10* expression, emanating from central (and possibly hypaxial) somites is one of the earliest crucial regulators of mammary line initiation. Interestingly, a recent genome-wide association study found that variance in teat number in pigs was

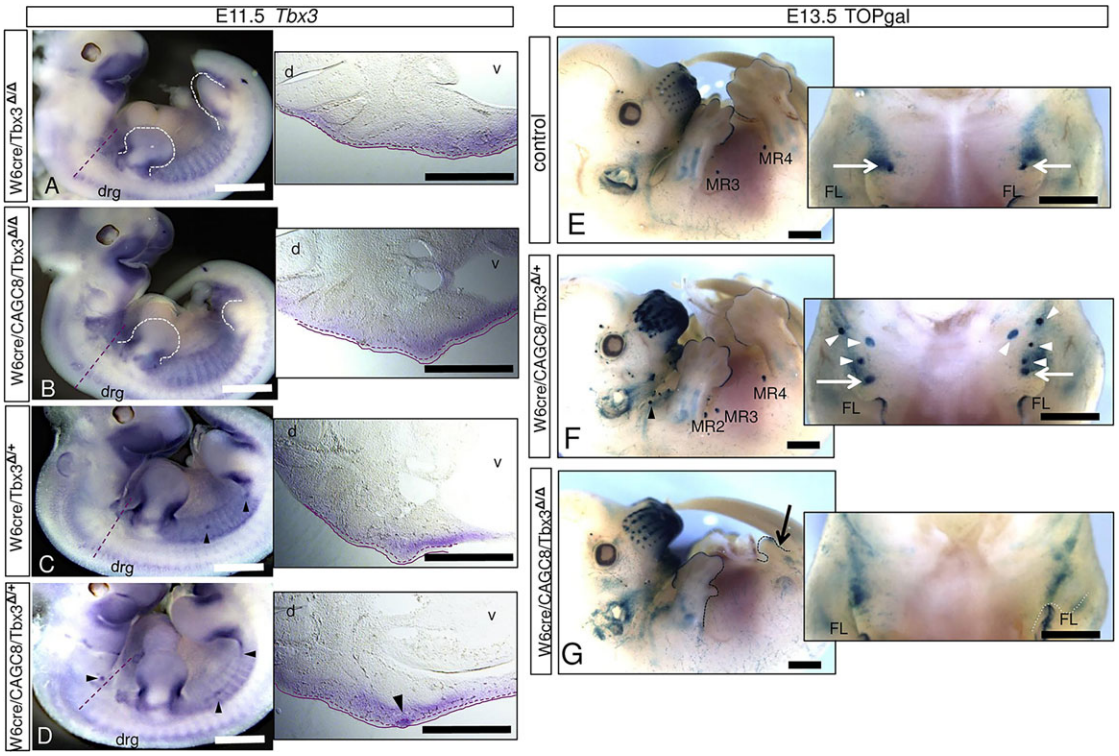

Fig. 7. Ectodermal ablation of *Tbx3* eliminates all MRs in W6cre/CAGC8 embryos. (A-D) *Tbx3* expression in E11.5 control (A,C) and W6cre/CAGC8 (B,D) embryos after conditional ablation of ectodermal *Tbx3*. Accompanying panels are 70 µm vibratome sections at the approximate sectioning planes indicated by the dashed lines. Dotted and solid lines in insets demarcate mesodermal and ectodermal boundaries, respectively. Mammary placodes form in control (C) and mutant (D) embryos when only a single *Tbx3* allele is conditionally ablated (arrowheads). (E-G) TOPgal expression in E13.5 control (E), W6cre/CAGC8/Tbx3$^{\Delta/+}$/TOPgal (F) and W6cre/CAGC8/Tbx3$^{\Delta/\Delta}$ /TOPgal (G) embryos. Accompanying panels are frontal views of the cervical region. White arrows point to the normal position of MR1. Arrowheads point to cervical MRs anterior to MR1. Loss of ectodermal *Tbx3* prevents MR formation (G) and leads to severe limb defects (arrow). Scale bars: 500 µm for vibratome sections in A-D; 1 mm in all other panels/insets.

Development (2015) 142, 4056-4067 doi:10.1242/dev.128298

significantly associated with quantitative trait loci containing genes involved in vertebral development and possibly back length (Duijvesteijn et al., 2014). This raises the possibility that a Hoxc8-induced transformation of cervical into thoracic vertebrae creates a new signaling zone for mammary gland induction. However, ectopic *Hoxc8* expression in Pax3cre/CAGC8 mutants produced completely penetrant cervical ribs without accompanying placode development in the cervical region. As these mutants often developed an additional MR along the normal mammary line, this suggests that somitic *Hoxc8* misexpression (even without accompanying ectodermal expression) produces alterations in signaling gradients that can be interpreted by an ectoderm that is already specified for mammary development, but that somitic factors expressed during the thoracic patterning program cannot independently potentiate mammary ectoderm in the cervical region.

Ectopic *Hoxc8* dysregulates mammary line Wnt signaling and placode patterning along the mammary line

Regulation of Wnt signaling by Hox factors has not been widely reported. However, as studies continue to uncover downstream targets of Hox genes, it is becoming apparent that this regulatory role of Hox genes has been overlooked. For example, using ChIP-seq, Donaldson et al. (2012) identified regions of the genome bound by Hoxa2 in the context of second branchial arch development. Of the thousands of genes identified, the majority fell within the Gene Ontology (GO) category of 'Wnt receptor signaling'. W6cre/CAGC8 mutants show mammary phenotypes with striking similarities to those of mice carrying targeted mutations of the Wnt pathway modulators *Sostdc1* (*Wise* or *Ectodin*) and *Lrp4* (Ahn et al., 2013; Närhi et al., 2012). Shared features between W6cre/CAGC8, *Sostdc1*$^{-/-}$ and *Lrp4* null mice are: delayed downregulation of Wnt signaling within mammary epithelium; larger diameter of mammary placodes; supernumerary embryonic MRs developing along the mammary line (however, *Sostdc1*$^{-/-}$ mutant nipples only appear at puberty); and increased proximity and occasional fusion of mammary buds 2 and 3, which often protrude abnormally from the ectoderm. In addition, loss of *Sostdc1* results in ectopic hair follicles developing within nipple tissue (Närhi et al., 2012). Ablation of the mesodermal mammary factor *Gli3* in mice also shows notable similarities to the W6cre/CAGC8 mammary phenotype, which is likely to be due to dysregulation of Wnt signaling and of the crosstalk between the Shh and Wnt pathways during mammary development (Hatsell and Cowin, 2006). Deletion of *Gli3* causes inappropriate encroachment of hair follicles close to MR2, which itself protrudes abnormally from *Gli3* mutant ectoderm, similar to cervical mammary placodes in W6cre/CAGC8 mutants. Interestingly, deletion of *Gli3* also prevents the normal regression of mammary buds in male mice, comparable to the persistence of male MRs within the anterior ectopic zone of W6cre/CAGC8 mice (Chandramouli et al., 2013; Hatsell and Cowin, 2006; Lee et al., 2011, 2013; Ulloa et al., 2007).

Supernumerary mammary placode development has previously been reported in experimental mice, but always within or near the wild-type mammary line, never in unique regions (Ahn et al., 2013; Chu et al., 2004; Howard et al., 2005; Mustonen et al., 2003). This difference between our and previous mouse models of mammary induction underscores the ability of ectopic *Hoxc8* to initiate a mammary program, thus altering mesenchymal-ectodermal communication at the earliest stages of mammary line potentiation. Hoxc8 misexpression in both somites and the overlying ectoderm enables the generation of a novel mammary zone followed by appropriate specification and early development of MRs up to the stage of ductal tree formation.

A model of *Hoxc8*-induced ectopic mammary development

A simplified model describing the role of ectopic *Hoxc8* in the potentiation of cervical mammary ectoderm is as follows (Fig. S5). Somitic *Hoxc8* expression upregulates somitic *Fgf10* expression, which is a likely early requirement for potentiation of the cervical mammary zone, similar to the requirement for somitic *Fgf10* for potentiation of the mammary line. However, somitic *Hoxc8* expression alone is insufficient to induce cervical placode development (as evidenced by the lack of cervical MRs in the Pax3cre/CAGC8 phenotype), indicating an additional requirement for *Hoxc8* expression in the overlying ectoderm (as evidenced by robust cervical MR development in the W6cre/CAGC8 phenotype). Ectodermal *Hoxc8* expression triggers upregulation of ectodermal *Tbx3* expression, possibly via direct transcriptional activation, but only in specific regions where *Tbx3* expression and Wnt signaling co-occur in the underlying mesoderm. Ectodermal *Tbx3* expression maintains Wnt signaling crucial for ectodermal mammary potentiation. Within this ectopic cervical zone, *Tbx3*-expressing cells migrate towards placode positions based on somitic signaling gradients of Fgf10 and levels of Wnt activators.

This model is consistent with the absence of mammary programs initiated in other regions of mutant ectoderm that express *Hoxc8* but lack either or both Wnt signaling and *Tbx3* in the underlying mesoderm. This model also predicts other regions of the W6cre/CAGC8 embryo in which ectodermal *Tbx3* upregulation was observed in association with Wnt signaling and *Hoxc8* expression, such as the whisker placodes, outer ear epidermis and eyelid conjunctiva (our unpublished observations). These structures all lie in regions beyond somitic signaling gradients and, although they were all defective, none exhibited evidence of MR development.

Hox genes and normal mammary placode development

Endogenous *Hoxc8* expression in E10.5 surface ectoderm is consistent with a scenario in which *Hoxc8* helps coordinate the induction of mammary line ectoderm, but must be downregulated as epithelial cells migrate into proper position with respect to signaling gradients of *Fgf10* expression, and to *Tbx3*, *Gli3* and other modulating factors that fine-tune the levels of Wnt signaling. Following mammary line potentiation, somitic *Hoxc8* is well positioned to regulate specification of the third mammary placode, which develops in ectoderm directly overlying hypaxial extensions of somites 15 and 16.

Neither the *Hoxc8* knockout nor *Hox8* paralog knockout mice have reported mammary defects (Le Mouellic et al., 1992; van den Akker et al., 2001), although skin appendages were not specifically investigated in these mutants. Nevertheless, the scarcity of skin and skin accessory organ phenotypes exhibited by Hox deletion mutants is likely to be due to genetic compensation (Rossi et al., 2015), particularly functional rescue by other members of the Hox family of transcription factors, many of which exhibit overlapping expression patterns in fetal and adult skin (Boucherat et al., 2013; Chen and Capecchi, 1999; Wellik and Capecchi, 2003). For this reason, the complementary approach of conditional misexpression/overexpression can be essential to unraveling developmental mechanisms that involve complex transcriptional programs and signaling pathways mediated by Hox genes and members of other large gene family networks. We suspect that myriad combinations of Hox transcription factors involved in placode patterning might provide the source of copious regional flexibility of cutaneous accessory organs that we see within and across taxa. However, it remains to be determined whether other Hox genes exhibit early transient activation within relevant ectodermal domains.

Development (2015) 142, 4056-4067 doi:10.1242/dev.128298

MATERIALS AND METHODS

Animals and genotyping

CAGC8 founders, as well as *Cre* driver lines Hoxc8IresCre (C8cre) (Chen et al., 2010), Hoxa3IresCre (A3cre) (Macatee et al., 2003), Wnt6IresCre (W6cre) (N. Makki, PhD Thesis, University of Utah, 2010), Pax3cre (Engleka et al., 2005), the reporter lines RosalacZ, RosaYFP (Soriano, 1999) and TOPgal (DasGupta and Fuchs, 1999), and a $Tbx3^{flox}$ conditional knockout line (Frank et al., 2013) were maintained on C57BL/6 or C57BL/6×CD1 genomic backgrounds. Mice and embryos were genotyped by PCR. To create experimental and control embryos for analysis, A3cre, Pax3cre or Wnt6cre males were bred to CAGC8 females to create control and double-heterozygote mutant littermates. Mutant and controls were easily distinguished by GFP signal using a fluorescent lamp. To generate control and W6cre/CAGC8 embryos with one or two conditionally ablated copies of *Tbx3* in the *Wnt6* domain, *CAGC8/+;*$Tbx3^{flox/+}$ or *CAGC8/+;*$Tbx3^{flox/flox}$ dams were bred to *W6cre/+;*$Tbx3^{\Delta/+}$*;TOPgal/+* males. These males were morphologically and reproductively indistinguishable from littermates carrying no *Cre* allele. For further information on the construction and targeting of the conditional *Hoxc8* misexpression allele see the supplementary Materials and Methods. All mouse experiments were approved by the Institutional Animal Care and Use Committee of the University of Utah.

Immunohistochemistry

Embryos were fixed at 4°C in 4% paraformaldehyde in PBS for 1-5 days (for paraffin embedding), or up to 24 h (for OCT embedding). Primary antibodies used for this study were: Hoxc8 (1:200; Covance, MMS-286R), Tbx3 (1:200; a generous gift from A. Moon, University of Utah), Lef1 (1:1000; Cell Signaling, 2230), AR (1:200; Millipore, 06-680) and ERα (1:200; Santa Cruz Biotechnology, sc-7207). For further details, see the supplementary Materials and Methods.

lacZ staining

Detection of β-gal reporter expression (RosalacZ or TOPgal) was performed as described in the supplementary Materials and Methods.

Whole-mount *in situ* hybridization

In situ hybridization was performed according to published protocols (Boulet and Capecchi, 1996). For details, see the supplementary Materials and Methods.

Chromatin immunoprecipitation (ChIP)

The ChIP procedure that we employed was a modification of a Jove video protocol developed for E8.5 embryos (Cho et al., 2011). For details of the protocol, see the supplementary Materials and Methods and Table S1.

Acknowledgements

We thank Sheila Barnett, Carol Lenz, Karl Lustig and the animal care staff of the Comparative Medicine Center at the University of Utah for technical assistance; Anne Moon for providing the *Tbx3* conditional mutant mouse; Anne Boulet and Matthew Hockin for critical reading of earlier versions of this manuscript; and Amir Pozner, Uchenna Emechebe and members of the M.R.C. lab for insightful discussion.

Competing interests

The authors declare no competing or financial interests.

Author contributions

L.S.C. developed the project and performed all experiments, data analysis and manuscript preparation. M.R.C. provided discussion and edited earlier versions of the manuscript.

Funding

This work was funded by the Howard Hughes Medical Institute and by the National Science Foundation (NSF) [grant 2R01HD030701-19]. Deposited in PMC for release after 6 months.

Supplementary information

Supplementary information available online at
http://dev.biologists.org/lookup/suppl/doi:10.1242/dev.128298/-/DC1

References

Ahn, Y., Sims, C., Logue, J. M., Weatherbee, S. D. and Krumlauf, R. (2013). Lrp4 and Wise interplay controls the formation and patterning of mammary and other skin appendage placodes by modulating Wnt signaling. *Development* **140**, 583-593.

Andl, T., Reddy, S. T., Gaddapara, T. and Millar, S. E. (2002). WNT signals are required for the initiation of hair follicle development. *Dev. Cell* **2**, 643-653.

Awgulewitsch, A. (2003). Hox in hair growth and development. *Naturwissenschaften* **90**, 193-211.

Bamshad, M., Le, T., Watkins, W. S., Dixon, M. E., Kramer, B. E., Roeder, A. D., Carey, J. C., Root, S., Schinzel, A., Van Maldergem, L. et al. (1999). The spectrum of mutations in TBX3: genotype/phenotype relationship in ulnar-mammary syndrome. *Am. J. Hum. Genet.* **64**, 1550-1562.

Bieberich, C. J., Ruddle, F. H. and Stenn, K. S. (1991). Differential expression of the Hox 3.1 gene in adult mouse skin. *Ann. N. Y. Acad. Sci.* **642**, 346-353; discussion 353-344.

Bitgood, M. J. and McMahon, A. P. (1995). Hedgehog and Bmp genes are coexpressed at many diverse sites of cell–cell interaction in the mouse embryo. *Dev. Biol.* **172**, 126-138.

Boras-Granic, K. and Hamel, P. A. (2013). Wnt-signalling in the embryonic mammary gland. *J. Mammary Gland Biol. Neoplasia* **18**, 155-163.

Boucherat, O., Montaron, S., Berube-Simard, F.-A., Aubin, J., Philippidou, P., Wellik, D. M., Dasen, J. S. and Jeannotte, L. (2013). Partial functional redundancy between Hoxa5 and Hoxb5 paralog genes during lung morphogenesis. *Am. J. Physiol. Lung Cell Mol. Physiol.* **304**, L817-L830.

Boulet, A. M. and Capecchi, M. R. (1996). Targeted disruption of hoxc-4 causes esophageal defects and vertebral transformations. *Dev. Biol.* **177**, 232-249.

Carapuço, M., Novoa, A., Bobola, N. and Mallo, M. (2005). Hox genes specify vertebral types in the presomitic mesoderm. *Genes Dev.* **19**, 2116-2121.

Chandramouli, A., Hatsell, S. J., Pinderhughes, A., Koetz, L. and Cowin, P. (2013). Gli activity is critical at multiple stages of embryonic mammary and nipple development. *PLoS ONE* **8**, e79845.

Chen, F. and Capecchi, M. R. (1999). Paralogous mouse Hox genes, Hoxa9, Hoxb9, and Hoxd9, function together to control development of the mammary gland in response to pregnancy. *Proc. Natl. Acad. Sci. USA* **96**, 541-546.

Chen, H. and Sukumar, S. (2003). Role of homeobox genes in normal mammary gland development and breast tumorigenesis. *J. Mammary Gland Biol. Neoplasia* **8**, 159-175.

Chen, S. C., Tvrdik, P., Peden, E., Cho, S., Wu, S., Spangrude, G. and Capecchi, M. R. (2010). Hematopoietic origin of pathological grooming in Hoxb8 mutant mice. *Cell* **141**, 775-785.

Cho, K.-W., Kim, J.-Y., Song, S.-J., Farrell, E., Eblaghie, M. C., Kim, H.-J., Tickle, C. and Jung, H.-S. (2006). Molecular interactions between Tbx3 and Bmp4 and a model for dorsoventral positioning of mammary gland development. *Proc. Natl. Acad. Sci. USA* **103**, 16788-16793.

Cho, O. H., Rivera-Pérez, J. A. and Imbalzano, A. N. (2011). Chromatin immunoprecipitation assay for tissue-specific genes using early-stage mouse embryos. *J. Vis. Exp.*, e2677.

Cho, K.-W., Kwon, H.-J., Shin, J.-O., Lee, J.-M., Cho, S.-W., Tickle, C. and Jung, H.-S. (2012). Retinoic acid signaling and the initiation of mammary gland development. *Dev. Biol.* **365**, 259-266.

Chu, E. Y., Hens, J., Andl, T., Kairo, A., Yamaguchi, T. P., Brisken, C., Glick, A., Wysolmerski, J. J. and Millar, S. E. (2004). Canonical WNT signaling promotes mammary placode development and is essential for initiation of mammary gland morphogenesis. *Development* **131**, 4819-4829.

Chuong, C.-M. (1993). The making of a feather: homeoproteins, retinoids and adhesion molecules. *Bioessays* **15**, 513-521.

Cowin, P. and Wysolmerski, J. (2010). Molecular mechanisms guiding embryonic mammary gland development. *Cold Spring Harb. Perspect. Biol.* **2**, a003251.

DasGupta, R. and Fuchs, E. (1999). Multiple roles for activated LEF/TCF transcription complexes during hair follicle development and differentiation. *Development* **126**, 4557-4568.

Davenport, T. G., Jerome-Majewska, L. A. and Papaioannou, V. E. (2003). Mammary gland, limb and yolk sac defects in mice lacking Tbx3, the gene mutated in human ulnar mammary syndrome. *Development* **130**, 2263-2273.

Donaldson, I. J., Amin, S., Hensman, J. J., Kutejova, E., Rattray, M., Lawrence, N., Hayes, A., Ward, C. M. and Bobola, N. (2012). Genome-wide occupancy links Hoxa2 to Wnt-beta-catenin signaling in mouse embryonic development. *Nucleic Acids Res.* **40**, 3990-4001.

Duijvesteijn, N., Veltmaat, J. M., Knol, E. F. and Harlizius, B. (2014). High-resolution association mapping of number of teats in pigs reveals regions controlling vertebral development. *BMC Genomics* **15**, 542.

Eblaghie, M. C., Song, S.-J., Kim, J.-Y., Akita, K., Tickle, C. and Jung, H.-S. (2004). Interactions between FGF and Wnt signals and Tbx3 gene expression in mammary gland initiation in mouse embryos. *J. Anat.* **205**, 1-13.

Engleka, K. A., Gitler, A. D., Zhang, M., Zhou, D. D., High, F. A. and Epstein, J. A. (2005). Insertion of Cre into the Pax3 locus creates a new allele of Splotch and identifies unexpected Pax3 derivatives. *Dev. Biol.* **280**, 396-406.

Frank, D. U., Emechebe, U., Thomas, K. R. and Moon, A. M. (2013). Mouse TBX3 mutants suggest novel molecular mechanisms for Ulnar-mammary syndrome. *PLoS ONE* **8**, e67841.
Gallego, M. I., Beachy, P. A., Hennighausen, L. and Robinson, G. W. (2002). Differential requirements for shh in mammary tissue and hair follicle morphogenesis. *Dev. Biol.* **249**, 131-139.
Garcia-Gasca, A. and Spyropoulos, D. D. (2000). Differential mammary morphogenesis along the anteroposterior axis in Hoxc6 gene targeted mice. *Dev. Dyn.* **219**, 261-276.
Godwin, A. R. and Capecchi, M. R. (1998). Hoxc13 mutant mice lack external hair. *Genes Dev.* **12**, 11-20.
Hatsell, S. J. and Cowin, P. (2006). Gli3-mediated repression of Hedgehog targets is required for normal mammary development. *Development* **133**, 3661-3670.
Hayashida, T., Takahashi, F., Chiba, N., Brachtel, E., Takahashi, M., Godin-Heymann, N., Gross, K. W., Vivanco, M. d. M., Wijendran, V., Shioda, T. et al. (2010). HOXB9, a gene overexpressed in breast cancer, promotes tumorigenicity and lung metastasis. *Proc. Natl. Acad. Sci. USA* **107**, 1100-1105.
Howard, B. A. (2008). The role of NRG3 in mammary development. *J. Mammary Gland Biol. Neoplasia* **13**, 195-203.
Howard, B., Panchal, H., McCarthy, A. and Ashworth, A. (2005). Identification of the scaramanga gene implicates Neuregulin3 in mammary gland specification. *Genes Dev.* **19**, 2078-2090.
Ikeya, M. and Takada, S. (1998). Wnt signaling from the dorsal neural tube is required for the formation of the medial dermomyotome. *Development* **125**, 4969-4976.
Johansson, J. A. and Headon, D. J. (2014). Regionalisation of the skin. *Semin. Cell Dev. Biol.* **25-26**, 3-10.
Jung, H.-S., Oropeza, V. and Thesleff, I. (1999). Shh, Bmp-2, Bmp-4 and Fgf-8 are associated with initiation and patterning of mouse tongue papillae. *Mech. Dev.* **81**, 179-182.
Kanzler, B., Viallet, J. P., Le Mouellic, H., Boncinelli, E., Duboule, D. and Dhouailly, D. (1994). Differential expression of two different homeobox gene families during mouse tegument morphogenesis. *Int. J. Dev. Biol.* **38**, 633-640.
Kanzler, B., Prin, F., Thelu, J. and Dhouailly, D. (1997). CHOXC-8 and CHOXD-13 expression in embryonic chick skin and cutaneous appendage specification. *Dev. Dyn.* **210**, 274-287.
Kessel, M. and Gruss, P. (1991). Homeotic transformations of murine vertebrae and concomitant alteration of Hox codes induced by retinoic acid. *Cell* **67**, 89-104.
Le Mouellic, H., Lallemand, Y. and Brûlet, P. (1992). Homeosis in the mouse induced by a null mutation in the Hox-3.1 gene. *Cell* **69**, 251-264.
Lee, M. Y., Racine, V., Jagadpramana, P., Sun, L., Yu, W., Du, T., Spencer-Dene, B., Rubin, N., Le, L., Ndiaye, D. et al. (2011). Ectodermal influx and cell hypertrophy provide early growth for all murine mammary rudiments, and are differentially regulated among them by Gli3. *PLoS ONE* **6**, e26242.
Lee, M. Y., Sun, L. and Veltmaat, J. M. (2013). Hedgehog and Gli signaling in embryonic mammary gland development. *J. Mammary Gland Biol. Neoplasia* **18**, 133-138.
Lewis, M. T. (2000). Homeobox genes in mammary gland development and neoplasia. *Breast Cancer Res.* **2**, 158-169.
Lim, X. and Nusse, R. (2013). Wnt signaling in skin development, homeostasis, and disease. *Cold Spring Harb. Perspect. Biol.* **5**, pii: a008029.
Macatee, T. L., Hammond, B. P., Arenkiel, B. R., Francis, L., Frank, D. U. and Moon, A. M. (2003). Ablation of specific expression domains reveals discrete functions of ectoderm- and endoderm-derived FGF8 during cardiovascular and pharyngeal development. *Development* **130**, 6361-6374.
Mailleux, A. A., Spencer-Dene, B., Dillon, C., Ndiaye, D., Savona-Baron, C., Itoh, N., Kato, S., Dickson, C., Thiery, J. P. and Bellusci, S. (2002). Role of FGF10/FGFR2b signaling during mammary gland development in the mouse embryo. *Development* **129**, 53-60.
McIntyre, D. C., Rakshit, S., Yallowitz, A. R., Loken, L., Jeannotte, L., Capecchi, M. R. and Wellik, D. M. (2007). Hox patterning of the vertebrate rib cage. *Development* **134**, 2981-2989.
Mentzer, S. E., Sundberg, J. P., Awgulewitsch, A., Chao, H. H. J., Carpenter, D. A., Zhang, W.-D., Rinchik, E. M. and You, Y. (2008). The mouse hairy ears mutation exhibits an extended growth (anagen) phase in hair follicles and altered Hoxc gene expression in the ears. *Vet. Dermatol.* **19**, 358-367.
Mikkola, M. L. (2007). Genetic basis of skin appendage development. *Semin. Cell Dev. Biol.* **18**, 225-236.
Mikkola, M. L. and Millar, S. E. (2006). The mammary bud as a skin appendage: unique and shared aspects of development. *J. Mammary Gland Biol. Neoplasia* **11**, 187-203.
Mustonen, T., Pispa, J., Mikkola, M. L., Pummila, M., Kangas, A. T., Pakkasjärvi, L., Jaatinen, R. and Thesleff, I. (2003). Stimulation of ectodermal organ development by Ectodysplasin-A1. *Dev. Biol.* **259**, 123-136.
Mustonen, T., Ilmonen, M., Pummila, M., Kangas, A. T., Laurikkala, J., Jaatinen, R., Pispa, J., Gaide, O., Schneider, P., Thesleff, I. et al. (2004). Ectodysplasin A1 promotes placodal cell fate during early morphogenesis of ectodermal appendages. *Development* **131**, 4907-4919.
Närhi, K., Tummers, M., Ahtiainen, L., Itoh, N., Thesleff, I. and Mikkola, M. L. (2012). Sostdc1 defines the size and number of skin appendage placodes. *Dev. Biol.* **364**, 149-161.
Petiot, A., Conti, F. J. A., Grose, R., Revest, J.-M., Hodivala-Dilke, K. M. and Dickson, C. (2003). A crucial role for Fgfr2-IIIb signalling in epidermal development and hair follicle patterning. *Development* **130**, 5493-5501.
Phippard, D. J., Weber-Hall, S. J., Sharpe, P. T., Naylor, M. S., Jayatalake, H., Maas, R., Woo, I., Roberts-Clark, D., Francis-West, P. H., Liu, Y. H. et al. (1996). Regulation of Msx-1, Msx-2, Bmp-2 and Bmp-4 during foetal and postnatal mammary gland development. *Development* **122**, 2729-2737.
Plikus, M., Wang, W. P., Liu, J., Wang, X., Jiang, T.-X. and Chuong, C.-M. (2004). Morpho-regulation of ectodermal organs: integument pathology and phenotypic variations in K14-Noggin engineered mice through modulation of bone morphogenic protein pathway. *Am. J. Pathol.* **164**, 1099-1114.
Pollock, R. A., Jay, G. and Bieberich, C. J. (1992). Altering the boundaries of Hox3.1 expression: evidence for antipodal gene regulation. *Cell* **71**, 911-923.
Propper, A. Y. (1978). Wandering epithelial cells in the rabbit embryo milk line. A preliminary scanning electron microscope study. *Dev. Biol.* **67**, 225-231.
Reid, A. I. and Gaunt, S. J. (2002). Colinearity and non-colinearity in the expression of Hox genes in developing chick skin. *Int. J. Dev. Biol.* **46**, 209-215.
Rossi, A., Kontarakis, Z., Gerri, C., Nolte, H., Hölper, S. Krüger, M. and Stainer, D. Y. R. (2015). Genetic compensation induced by deleterious mutations but not gene knockdowns. *Nature* **524**, 230-233.
Soriano, P. (1999). Generalized lacZ expression with the ROSA26 Cre reporter strain. *Nat. Genet.* **21**, 70-71.
St-Jacques, B., Dassule, H. R., Karavanova, I., Botchkarev, V. A., Li, J., Danielian, P. S., McMahon, J. A., Lewis, P. M., Paus, R. and McMahon, A. P. (1998). Sonic hedgehog signaling is essential for hair development. *Curr. Biol.* **8**, 1058-1069.
Suzuki, K., Yamaguchi, Y., Villacorte, M., Mihara, K., Akiyama, M., Shimizu, H., Taketo, M. M., Nakagata, N., Tsukiyama, T., Yamaguchi, T. P. et al. (2009). Embryonic hair follicle fate change by augmented beta-catenin through Shh and Bmp signaling. *Development* **136**, 367-372.
Ulloa, F., Itasaki, N. and Briscoe, J. (2007). Inhibitory Gli3 activity negatively regulates Wnt/beta-catenin signaling. *Curr. Biol.* **17**, 545-550.
van den Akker, E., Fromental-Ramain, C., de Graaff, W., Le Mouellic, H., Brulet, P., Chambon, P. and Deschamps, J. (2001). Axial skeletal patterning in mice lacking all paralogous group 8 Hox genes. *Development* **128**, 1911-1921.
Veltmaat, J. M. (2013). Investigating molecular mechanisms of embryonic mammary gland development by bead-implantation in embryonic flank explant cultures – a protocol. *J. Mammary Gland Biol. Neoplasia* **18**, 247-252.
Veltmaat, J. M., Van Veelen, W., Thiery, J. P. and Bellusci, S. (2004). Identification of the mammary line in mouse by Wnt10b expression. *Dev. Dyn.* **229**, 349-356.
Veltmaat, J. M., Relaix, F., Le, L. T., Kratochwil, K., Sala, F. G., van Veelen, W., Rice, R., Spencer-Dene, B., Mailleux, A. A., Rice, D. P. et al. (2006). Gli3-mediated somitic Fgf10 expression gradients are required for the induction and patterning of mammary epithelium along the embryonic axes. *Development* **133**, 2325-2335.
Veltmaat, J. M., Ramsdell, A. F. and Sterneck, E. (2013). Positional variations in mammary gland development and cancer. *J. Mammary Gland Biol. Neoplasia* **18**, 179-188.
Wellik, D. M. and Capecchi, M. R. (2003). Hox10 and Hox11 genes are required to globally pattern the mammalian skeleton. *Science* **301**, 363-367.
Wu, X., Chen, H., Parker, B., Rubin, E., Zhu, T., Lee, J. S., Argani, P. and Sukumar, S. (2006). HOXB7, a homeodomain protein, is overexpressed in breast cancer and confers epithelial-mesenchymal transition. *Cancer Res.* **66**, 9527-9534.
Zhang, Y., Tomann, P., Andl, T., Gallant, N. M., Huelsken, J., Jerchow, B., Birchmeier, W., Paus, R., Piccolo, S., Mikkola, M. L. et al. (2009). Reciprocal requirements for EDA/EDAR/NF-kappaB and Wnt/beta-catenin signaling pathways in hair follicle induction. *Dev. Cell* **17**, 49-61.

Supplementary Materials and Methods

Constructing and Targeting the Conditional Hoxc8 Misexpression Allele

To make the conditional RosaCAGGSHoxC8IresGFP allele (herein abbr. CAGC8), the *Hoxc8* open reading frame was PCR amplified from E11.5 whole embryo mouse cDNA and cloned into pCAGstop2 along with an IresEGFP casette. The plasmid was then placed into the 3' UTR of the Rosa locus. LoxP sites between the CAG promoter and coding sequence allowed *Cre*-mediated removal of a transcription stop (and PGK-neomycin selection cassette) resulting in expression of bicistronic *Hoxc8* and *GFP* messages. Double heterozygote offspring created by crossing dams carrying the CAGC8 overexpression allele with males harboring any *Cre* driver allele will express *Hoxc8* and *GFP* throughout the lineage of *Cre* expressing cells.

Immunohistochemistry and X-gal

Briefly, paraffin sections were dewaxed and rehydrated into water for five minutes before antigen retrieval (15-30 minute boil in 0.1 M citrate phosphate, pH 6.0). Sections were blocked for endogenous peroxidase in 0.1% H_2O_2. Primary antibodies were diluted in CytoQ solution and incubated on sections overnight at 4°C. Vector Elite ABC mouse or rabbit kits were used to amplify signal. Vector DAB (brown) or SG (black) kits were used with brief hematoxylin (Fisher) or nuclear fast red (Sigma) counterstain to visualize nuclear localization. Primary antibodies on frozen sections were treated as per paraffin sections, but a secondary antibody linked to alexa-fluor fluorescent reporter (Invitrogen) was used at 1:1000 for fluorescent imaging and DAPI was used as a nuclear counterstain. Fluorescent and bright field images were obtained with a M205FA microscope, using AF6000 imaging software (both Leica Microsystems).

Whole mount embryos carrying a beta-galactosidase reporter (RosaLacZ or TOPgal) were processed for 90 minutes in formalin/glutaraldehyde fixative before staining in X-gal solution (4 hours at RT° or up to 16 hours at 4°C). Post-fixed embryos were photographed before embedding for vibratome (70µ) sectioning (in agar), or for paraffin (10µ) sectioning (in paraplast). X-gal stained E10.75 C8cre/LacZ frozen sections were processed post-sectioning.

Whole-Mount In Situ Hybridization

Tbx3 and *Wnt10b* in situ hybridization probes were amplified from E11.5 mouse cDNA using the following primers: Tbx3F: 5'- TACTGAAACCGACTTCCAGGAG -3'. R: 5'-ACATTCTCTTTGGCATTTCGG-3'; Wnt10bF: 5'- TCACAGAGTGGGTCAATGTG-3', R: 5'- GTGACTCTTTCAGGTGCTCC-3'. Products were cloned into TOPOII dual promoter kit (Invitrogen K4500-01), linearized, then transcribed to make labeled antisense RNA probes using the appropriate polymerase with DIG RNA Labeling Kit (Roche 11 175 025 910). *Hoxc8*, *Myf5*, *Fgf10*, and *Bmp2* antisense probes were similarly prepared from frozen plasmid stock. All plasmids are available on request.

Chromatin Immunoprecipitation (ChIP)

In silico anaylsis (Kent et al., 2002) (http://genome.ucsc.edu/ ; Dec. 2011 GRCm38/mm10) was performed to identify putative *Hox* transcription factor binding sites contained within or near regions of evolutionary sequence conservation flanking and

intronic to the *Tbx3* coding sequence (Fig. 9B). Ten specific primer sets were designed to anneal at 60°C and amplify ten short (~150 bp) conserved or control regions (Table S1). The ChIP procedure we employed was a modification of a video protocol developed for E8.5 embryos, available at the Jove website (Cho et al., 2011). Briefly, E11.5 W6cre/CAGC8 and control embryos were harvested from CAGC8 females crossed to W6cre males. Lateral flank (mesoderm + ectoderm) and dorsal tissue (consisting of somites + neural tube) were separately collected. Left and right sides from three embryos were used to prepare flank and dorsal ChIP samples of each genotype (W6cre/CAGC8 and control). Tissue was disaggregated in Collagenase Type II (Gibco #17101-015). Approximately 5 X 10^6 cells were used for each chromatin preparation. Samples were cross-linked, washed in DPBS, and frozen at -80°C until further use.

Thawed cross-linked cells were suspended in 200 µL SDS lysis buffer (50 mM Tris-HCl (pH 8.1), 10 mM EDTA and 1% SDS) with freshly added PIC (Roche #11 836 170 001). These were sonicated (30 seconds on, 30 seconds off) for 30 cycles using an automated Diagenode bioruptor sonication system (B01010002). After centrifugation, 40 µL of each eluate was aliquoted into 5 equal volumes and frozen at -80°C until further use. Thawed sonicated samples were diluted in 400 µL ChIP dilution buffer (16.7 mM Tris-HCl (pH 8.1), 1.2 mM EDTA, 1.1% TritonX, 167 mM NaCl and 0.01% SDS). Immunoprecipitation (IP) and washing steps were performed with a Dynal MPC magnetic particle concentrator (Invitrogen 123-210), using magnetic Protein G dynabeads (Novex #10007D) which had been blocked with 5 mg/mL BSA fraction V, 20 mg/mL glycogen, and 20 mg/mL yeast tRNA. Half of each sample was IP'd with blocked beads and Hoxc8 antibody (Covance) and the other half with blocked beads and mouse IgG serum (Vector Laboratories). Chromatin-protein-bead complexes were washed twice in dialysis buffer at 4°C (50 mM Tris-Cl (pH 8.1), 2 mM EDTA), four times in ChIP wash buffer at 4°C (100 mM Tris-Cl (pH 8.0), 500 mM LiCl, 1% NP-40, 1% NaDOC), and once in TE at RT°. Chromatin was eluted with 2 x 150 µL elution buffer (50 mM $NaHCO_3$, 1% SDS) at 65°C. Chromatin cross-links were reversed (in ChIP samples as well as pre-IP input), by incubating samples for four hours at 65°C with 20 µL 5 M NaCl and 1 µL 10 mg/mL RNAseA. Chromatin was purified with Qiagen PCR columns and eluted in 50 µL Qiagen EB buffer. 40 cycle PCR reactions were seeded with 2 µL flank or dorsal chromatin. (Table S1). Only primer pair #5 amplified both flank and dorsal tissue that had been precipitated with Hoxc8 antibody, and failed to amplify mouse IgG precipitated chromatin. This primer pair was then successfully tested on chromatin obtained from W6cre/CAGC8 embryos.

Reference

Kent, W. J., Sugnet, C. W., Furey, T. S., Roskin, K. M., Pringle, T. H., Zahler, A. M. and Haussler, D. (2002). The human genome browser at UCSC. *Genome Res* **12**, 996-1006.

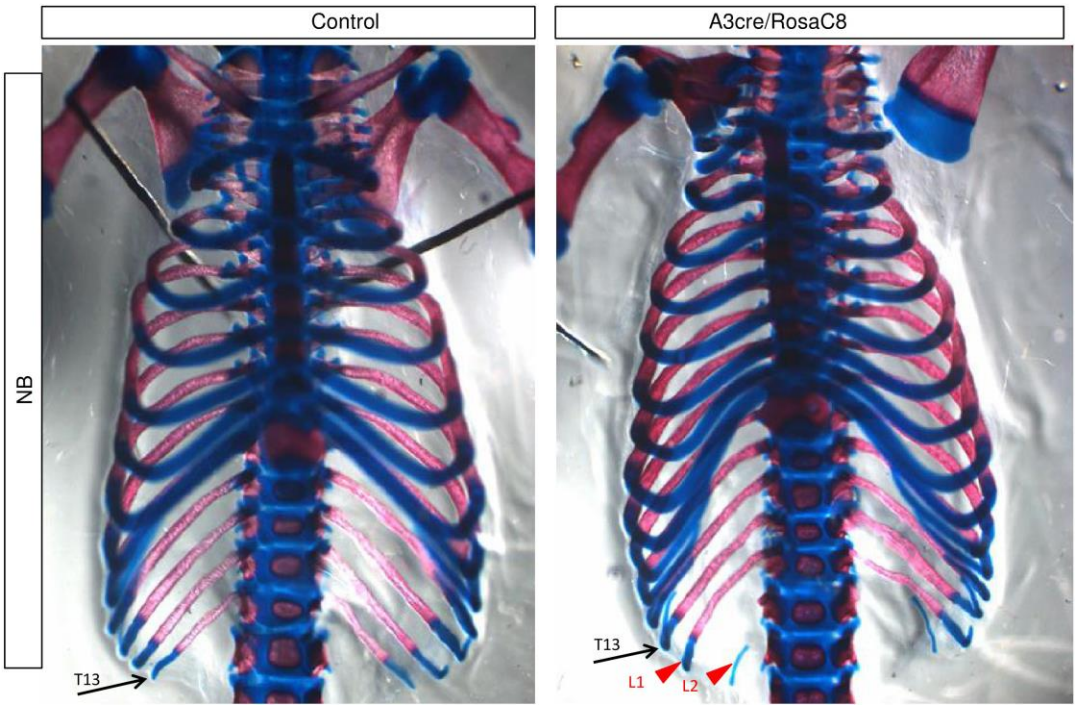

Figure S1
Ribs in newborn control and mutant mice generated from our initial *Hoxc8* conditional misexpression construct (crossed to Hoxa3IresCre). This initial construct lacked the CAGGS promoter and was instead driven by the endogenous Rosa promoter. Mutants survive until birth and have a considerably milder rib phenotype than A3cre/CAGC8 embryos. Arrows point to T13, arrowheads point to ectopic ribs on the first two lumbar vertebrae (T14 and T15).

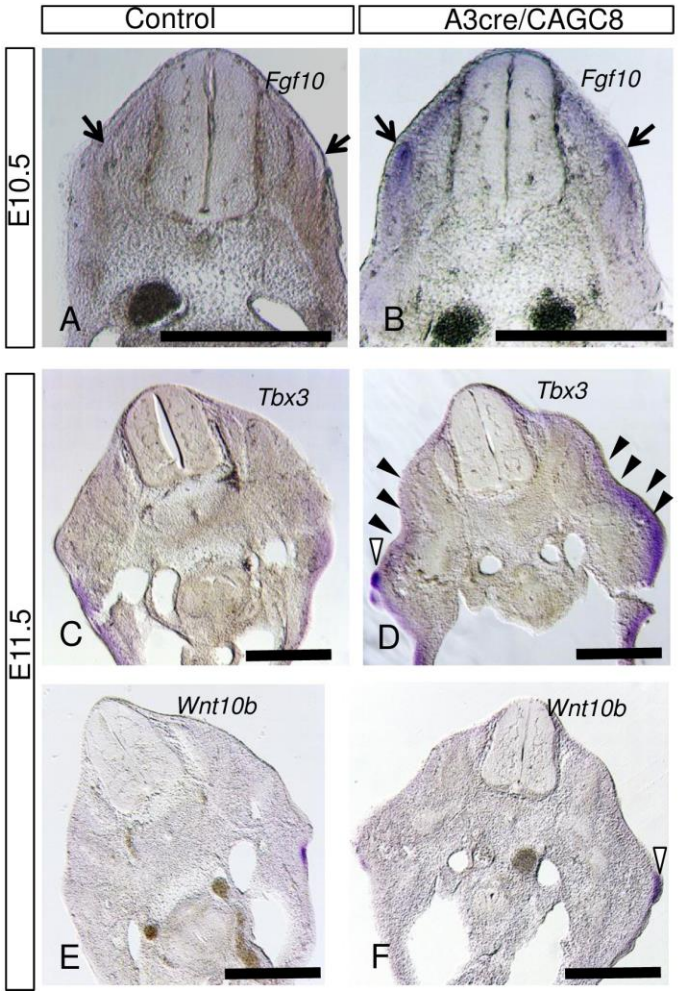

Figure S2
70 µm vibratome sections through the cervical region of whole mount control (A,C,E) and A3cre/CAGC8 (B,D,F) in situ embryos. **(A,B)** E10.5 embryos probed with *Fgf10*. Arrows indicate somitic upregulation in mutant. **(C,D)** E11.5 embryos probed with *Tbx3* black arrowheads indicate upregulated mesodermal signal in mutant. White arrowhead indicates an ectopic cervical placode. **(C,D)** E11.5 embryos probed with *Wnt10b*. Arrowhead indicates an ectopic cervical placode. Scale bars: 500µm.

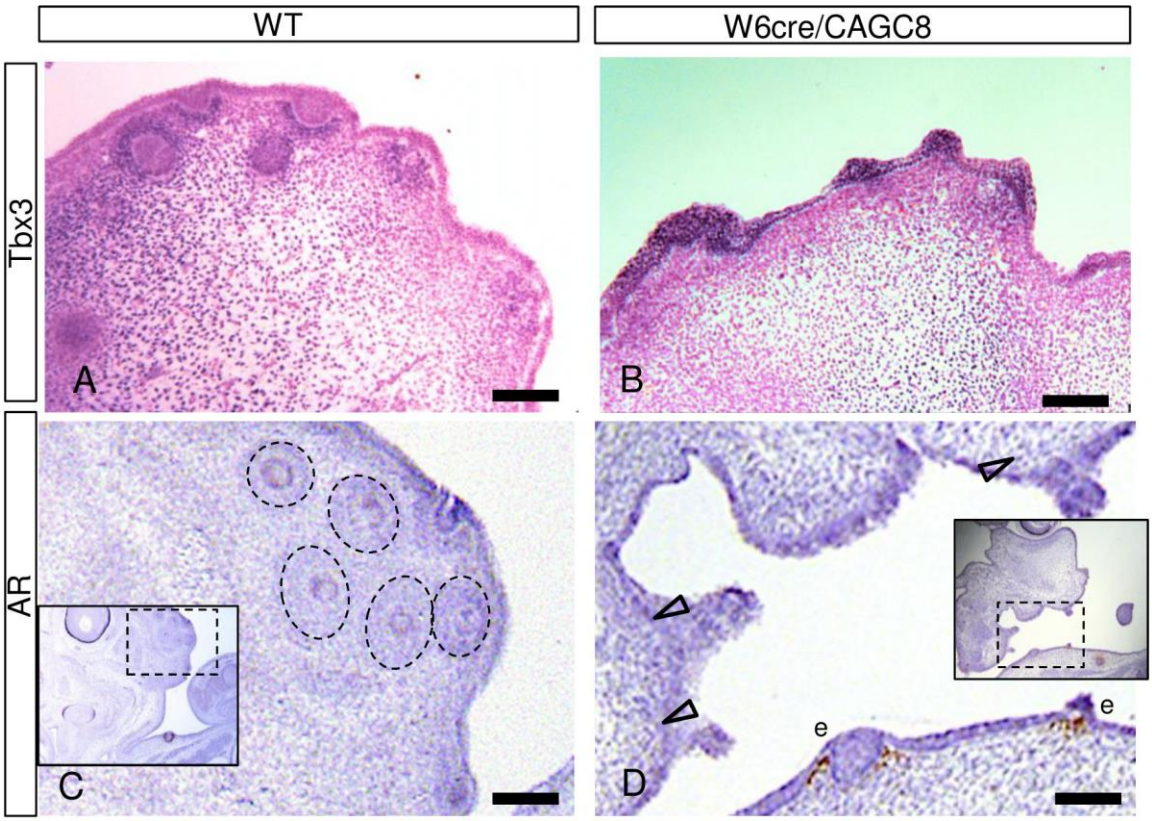

Figure S3
(A,B) Tbx3 is strongly upregulated in the ectoderm of defective W6cre/CAGC8 vibrissal placodes. **(C,D)** Lack of androgen receptor (AR) in mesenchyme of mutant vibrissae (open arrowheads) suggests defective vibissae are not reprogrammed towards a mammary fate. Scale bars: 100μm.

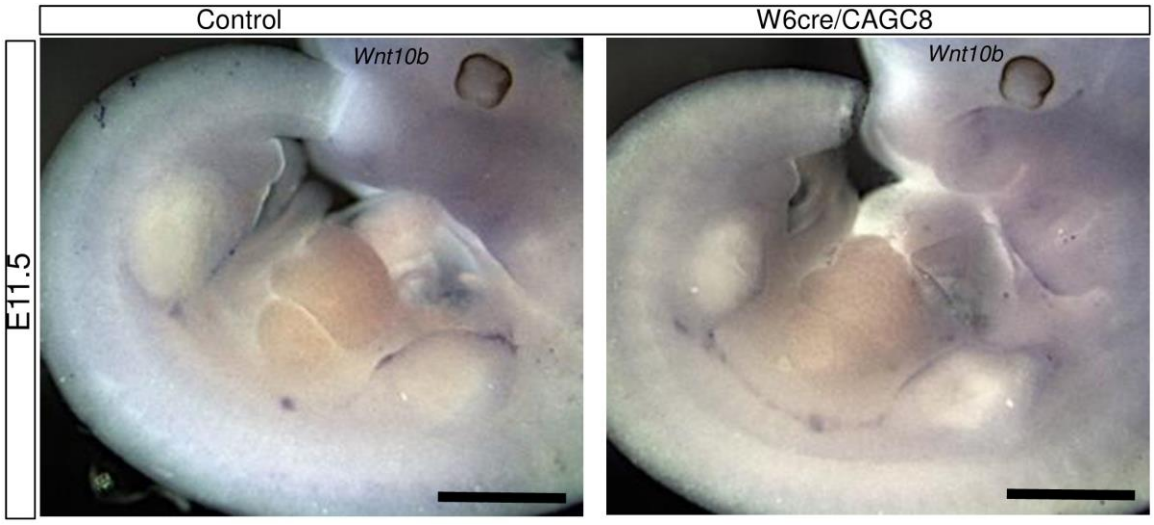

Figure S4
Delayed mammary placode assembly and lingering *Wnt10b* expression along the mammary line of an (early) E11.5 W6cre/CAGC8 embryo compared to a control littermate. Limbs are removed. Scale bars: 1mm

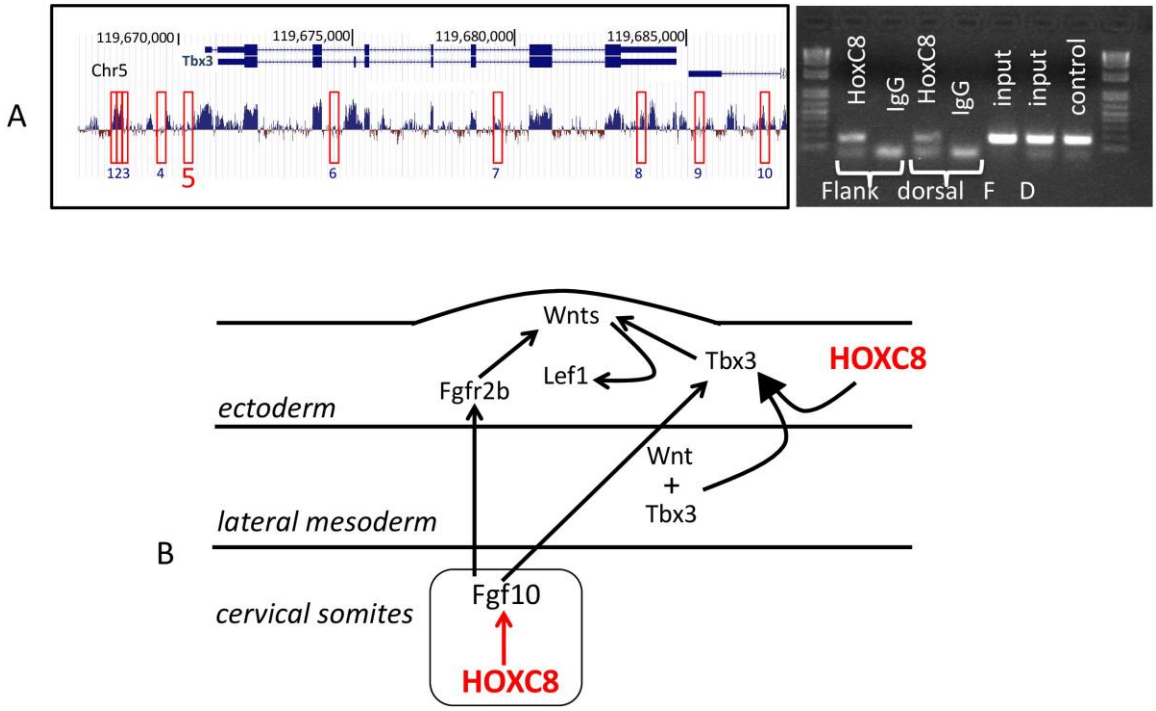

Figure S5

(A) Eight evolutionarily conserved genomic regions (excluding exons) designated by boxes 1, 2, 3, 5, 7, 8, 9, 10 and two non-conserved regions (boxes 4, 6) associated with the *Tbx3* locus were identified as carrying putative *Hox* transcription factor binding sites (see supplementary materials and methods). Polymerase chain reaction (PCR) amplified a region 1.5 Kb 5' of the *Tbx3* ATG start (region/primer set #5) from Hoxc8 antibody-immunoprecipitated tissue but not from mouse IgG serum-immunoprecipitated tissue of a W6cre/CAGC8 mutant. **(B)** Model of ectopic mammary placode formation requires somitic HoxC8 expression for induction of *Fgf10* and ectodermal Hoxc8 expression for induction of *Tbx3* (see results and discussion).

Table S1
Tbx3 primer sequences for ChIP. Only primer set #5 amplifies sequence bound to Hoxc8 antibody, but not to mouse IgG serum.

Primer set	Forward	reverse
1	5'-gccacaagcctaagcaagac-3'	gatcaaaagcaggaaggtgc
2	gcaccttcctgcttttgatcc	atcccagtttgccacttctc
3	agaagtggcaaactgggatg	gcatgcaaataatctggcct
4	caaaggtcttgtcccaggaa	cgatcagactttggttgggt
5	**cgcaggagctagaggatctg**	**tctgcagcttcttccctttc**
6	gaatgtggacagacagggct	tctgacttttcacccaggc
7	gtgtcagctttggggaggta	tcttccaccacaccctcttc
8	gggagatgaagtcctgtgga	ccagcatcggctcttaaaac
9	agtcccgagtcagttaggca	aggacaggacagaggcttca
10	gggctttagagctgtgggta	agcctacacaccgtacaccc